LA-UR-16-29061
Approved for public release; distribution is unlimited.

Title: Feasibility Study for Electrical Discharge Machining of Large DU-Mo Castings

Author(s): Hill, Mary Ann; Dombrowski, David E.; Clarke, Kester Diederik; Forsyth, Robert Thomas; Aikin, Robert M. Jr.; Alexander, David John; Tegtmeier, Eric Lee; Robison, Jeffrey Curt; Beard, Timothy Vance; Edwards, Randall Lynn; Mauro, Michael Ernest; Scott, Jeffrey E.; Strandy, Matthew Thomas

Intended for: Report

Issued: 2016-11-29

31 October, 2016

Feasibility Study for Electrical Discharge Machining of Large DU-Mo Castings

Final Report

Mary Ann Hill, Dave Dombrowski, Kester Clarke, Robert Forsyth, Rob Aikin, Dave Alexander, Eric Tegtmeier, Jeff Robison, Tim Beard, Randy Edwards, Mike Mauro, Jeff Scott, Matt Strandy

SIGMA Division

Los Alamos National Laboratory

Introduction

U-10 wt. % Mo (U-10Mo) alloys are being developed as low enrichment monolithic fuel for the CONVERT program. Optimization of processing for the monolithic fuel is being pursued with the use of electrical discharge machining (EDM) under CONVERT HPRR WBS 1.2.4.5 Optimization of Coupon Preparation. The process is applicable to manufacturing experimental fuel plate specimens for the Mini-Plate-1 (MP-1) irradiation campaign. The benefits of EDM are reduced machining costs, ability to achieve higher tolerances, stress-free, burr-free surfaces eliminating the need for milling, and the ability to machine complex shapes. Kerf losses are much smaller with EDM (tenths of mm) compared to conventional machining (mm). Reliable repeatability is achievable with EDM due to its computer generated machining programs.

Casting

A flow chart of processing the U-10Mo foils is shown in Figure 1. A depleted U-10Mo casting was made using a horizontal billet mold. The mold was developed under the VIM Casting Optimization Task from the Y-12 initial design. An HML grade graphite mold with yttria coating was used. The casting was made in Los Alamos National Laboratory's single coil vacuum induction melt (VIM) "C"-Furnace. The charge material consisted of arc-melted U-10Mo buttons, shown in Figure 2. The charge was 15.5 kg resulting in a casting of 13.6 kg. The casting yield was 88%. The casting procedure involved using a 55kW induction power level up to 1328^{o}C. The power was then cut and held at 1328^{o}C for ten minutes. The stopper rod was then pulled and the induction power was turned off. Figure 3 shows the location of the thermocouples during the casting. An image of the as-cast part is shown in Figure 4.

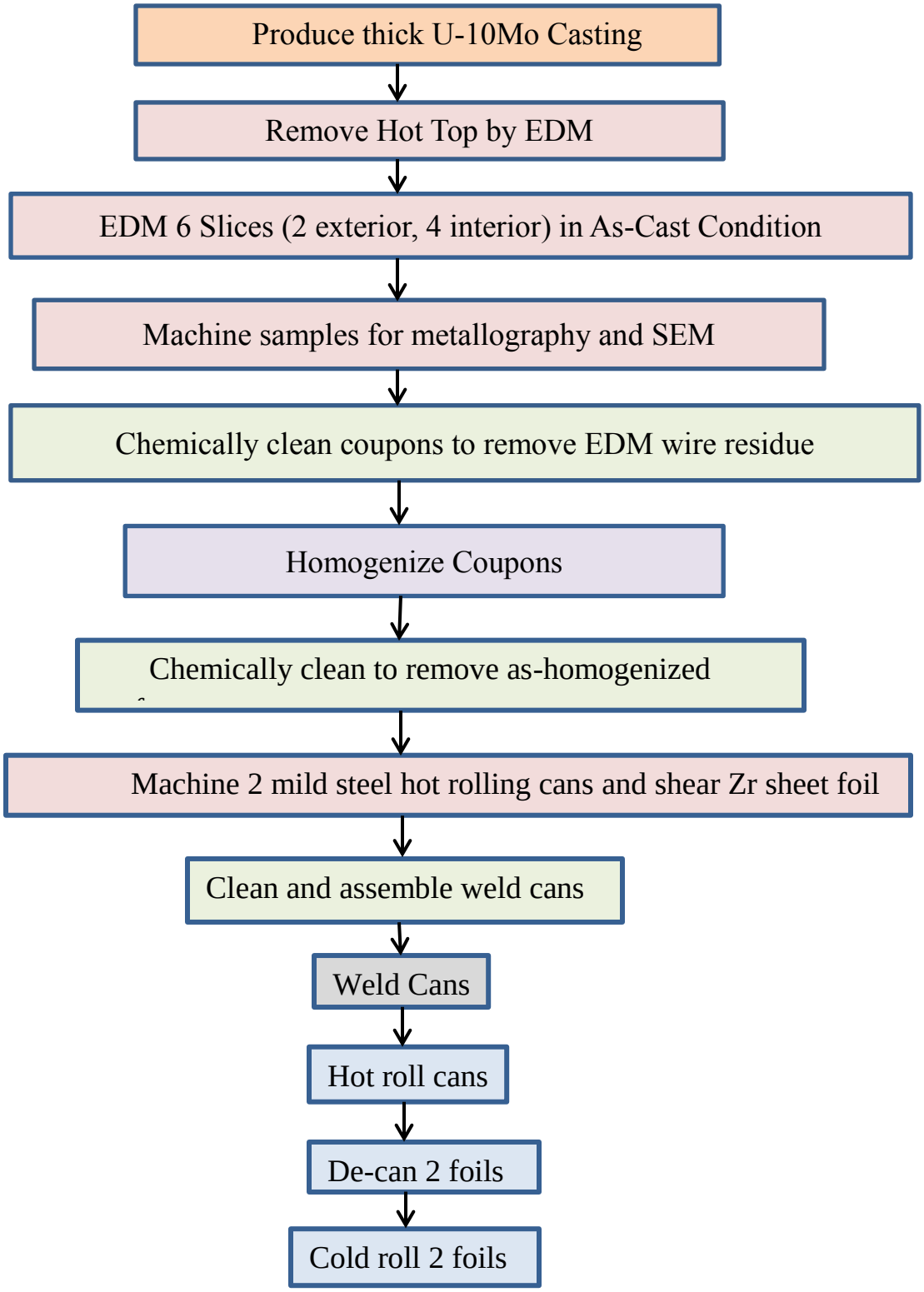

Figure 1. Processing of U-10Mo foils.

Figure 2. Arc-melted button charge in crucible for U-10Mo casting.

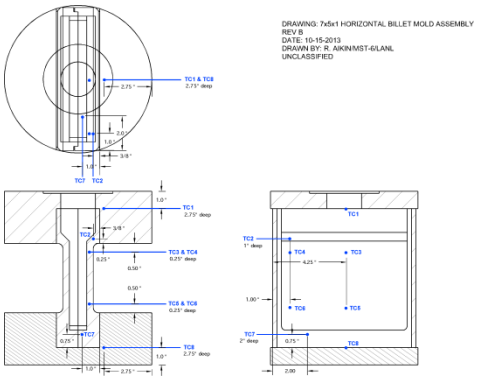

Figure 3. Thermocouple locations in casting.

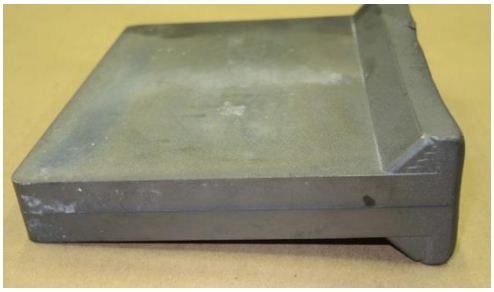

Figure 4. The U-10Mo casting with dimensions of 5.17”x 7.12”x 1.20” (131 mm x 181 mm x 30.5 mm).

Electrical Discharge Machining

The wire-electrical discharge machine used for this project was a Mitsubishi FA20V. Figure 4a and 4b show EDM of the U-10Mo casting. The casting was cut into six 1/8” (3.2 mm) thick slices, shown in Figure 5. Four coupons, 3” x 4” (76.2 mm x 101.6 mm), were subsequently machined from the slices. The EDM wire was 0.010 inch (0.25 mm) diameter brass. This diameter wire results in a kerf that is about 0.012 inches wide (0.30 mm). The dielectric fluid was deionized water. The fluid provides insulation against premature discharge, cools the machined area, and flushes away machining chips. Machining parameters are listed in Table 1. The weight of the slices is listed in Table 2 and a U-10Mo slice is shown in Figure 6. The 3” x 4” U-10Mo interior coupons weighed approximately 450 $\pm$ 5 grams following machining. The exterior slice used for this study weighed 580 grams. Milling of 0.040” (1 mm) from the surface adjacent to the graphite crucible was done to remove any reaction layer.

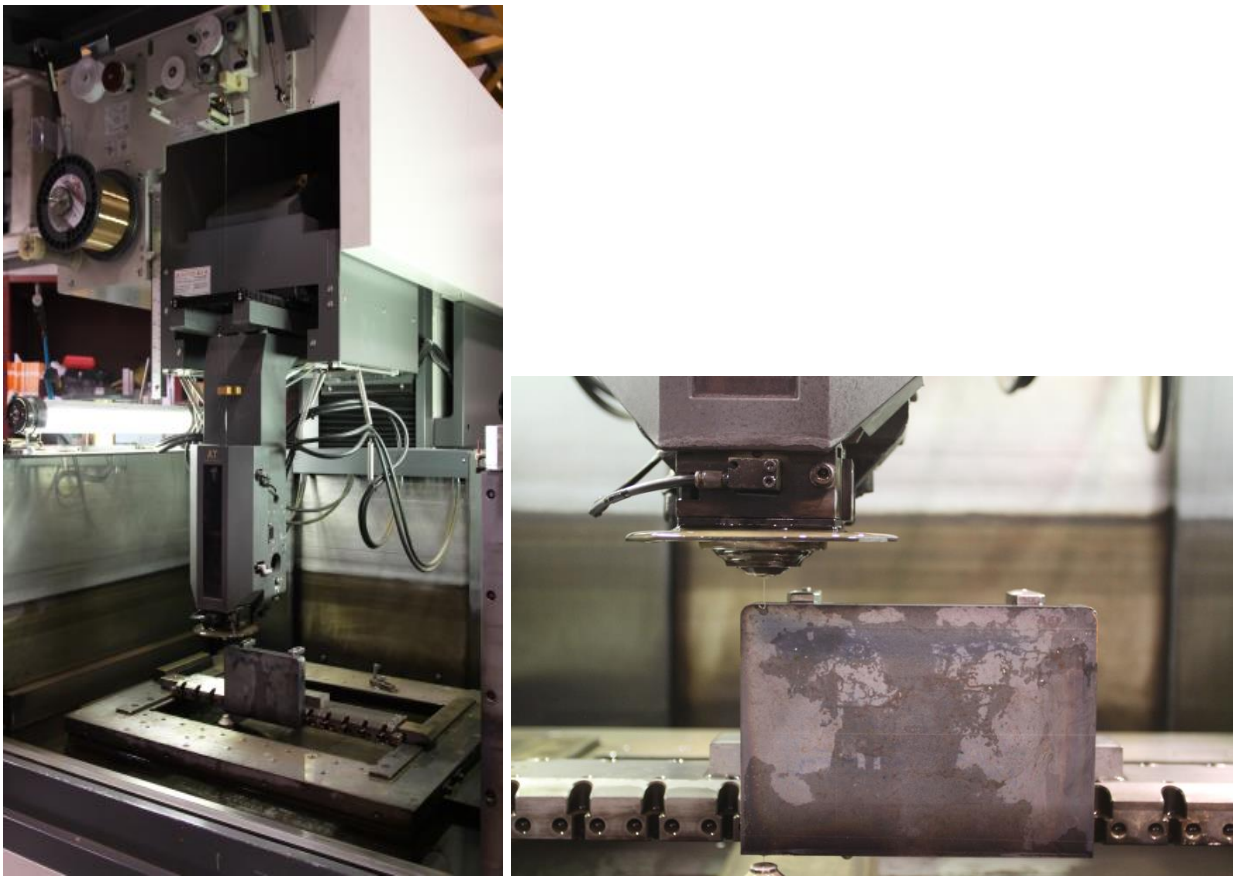

Figure 5. Left: EDM of U-10Mo casting with brass wire spool in upper left corner.
Right: Close-up of EDM of U-10Mo casting.

Table 1. Electrical Discharge Machining Parameters

Parameter	Description	Setting	Maximum Setting
Voltage Open (VO)	Set height of gap voltage when no load is applied	4	16
Power Setting (IP)	Size of peak current that flows through the gap (wire breakage occurs if set too high)	8	18
Delta Power (ΔIP)	Finely adjust size of peak current flowing through the gap	8	16
Off Time (Off)	Duration of rest pauses required for reionization of the dielectric – off time decreases for lower settings	1	16
Stability A (SA)	Determines machine stability by finely adjusting current (higher the value, faster the machining speed)	3	8
Stability B (SB)	Determines machining stability by finely adjusting off time	8	16
Stability C (SC)	Used to stabilize machining, particularly during rough machining	3	3
Stability E (SE)	Sets machining stability during first cut machining	4	5
Voltage Gap (VG)	Measurement of electrical voltage across the gap between the electrode and work piece. When the electrode is too far away to allow machining or current, this is called “open-gap voltage” and is very high (up to 300 V). During EDM machining, this is called “working gap voltage” and can be as low as 35 V.	60	150
Wire Speed (WS)	Wire feed rate (higher the value, the faster the rate)	8	16
Wire Tension (WT)	Wire tension (higher the value, stronger the tension)	9	16
Pre Tension (PT)	Wire pretension (higher the value, stronger the tension)	14	16
Liquid Quantity (LQ)	Dielectric fluid flow rate	14	16
Liquid Resistivity	The measurement of the specific resistance of the water dielectric	9	9

Table 2. Weight of slices following EDM.

Slice Designation	Weight (g)
13C-743-HT (hot top)	3370.8
13C-743 (adjacent to crucible)	1724.1
13C-743-E	1357.3
13C-743-D	1367.6
13C-743-C	1375.6
13C-743-B	1351.5
13C-743-A (adjacent to crucible)	2196.9

Figure 6. DU-10Mo section from casting. EDM produces straight machining edges with no distortion.

Removal of the Recast Layer

With EDM, electrical discharges are used to remove material from the work-piece. A spark can produce a temperature from 10,000-20,000^{o}C. One disadvantage of the EDM process is the formation of a recast layer at the machining interface. The thickness, composition, and condition of this layer depend on the discharge energy and composition of the work-piece, wire, and the dielectric fluid.[1] The thickness of the recast layer was approximately 12-16 microns, as shown in Figure 7. Energy-dispersive spectroscopy (EDS) was used to analyze the recast layer which is composed of copper and zinc from the brass wire, and oxides produced by the vaporizing water from the dielectric. This thin layer was removed with nitric acid. The recast layer can also be removed by milling or polishing. Figure 8 shows a line scan of the recast layer with small gray regions imbedded in the U-10Mo. This line scan suggests that oxygen is responsible for the

darker spots in the intermediate recast region between the primary recast layer and the uranium, as opposed to copper or zinc. X-ray maps, shown in Figure 9, were collected to show the discontinuity in the recast layer and the spotty occurrence of copper enrichment. The image is from a broad edge of the sample so the epoxy is at the top of the maps. The EDS spectra of the recast layer and an area with the recast layer removed are shown in Figures 10 and Fig. 11, respectively.

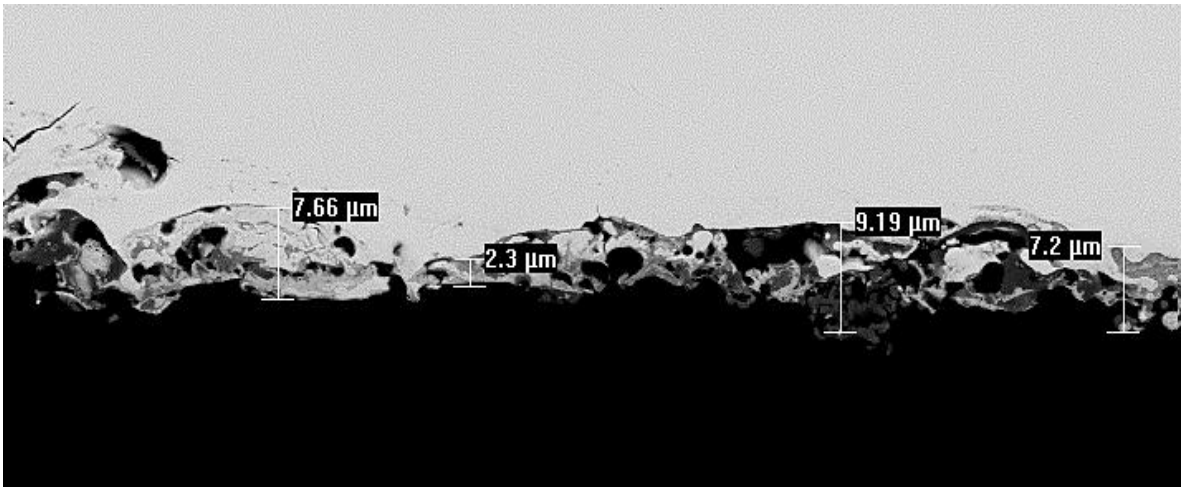

Figure 7. The recast layer on an interior slice of a U-10 wt. % Mo casting cut by EDM.

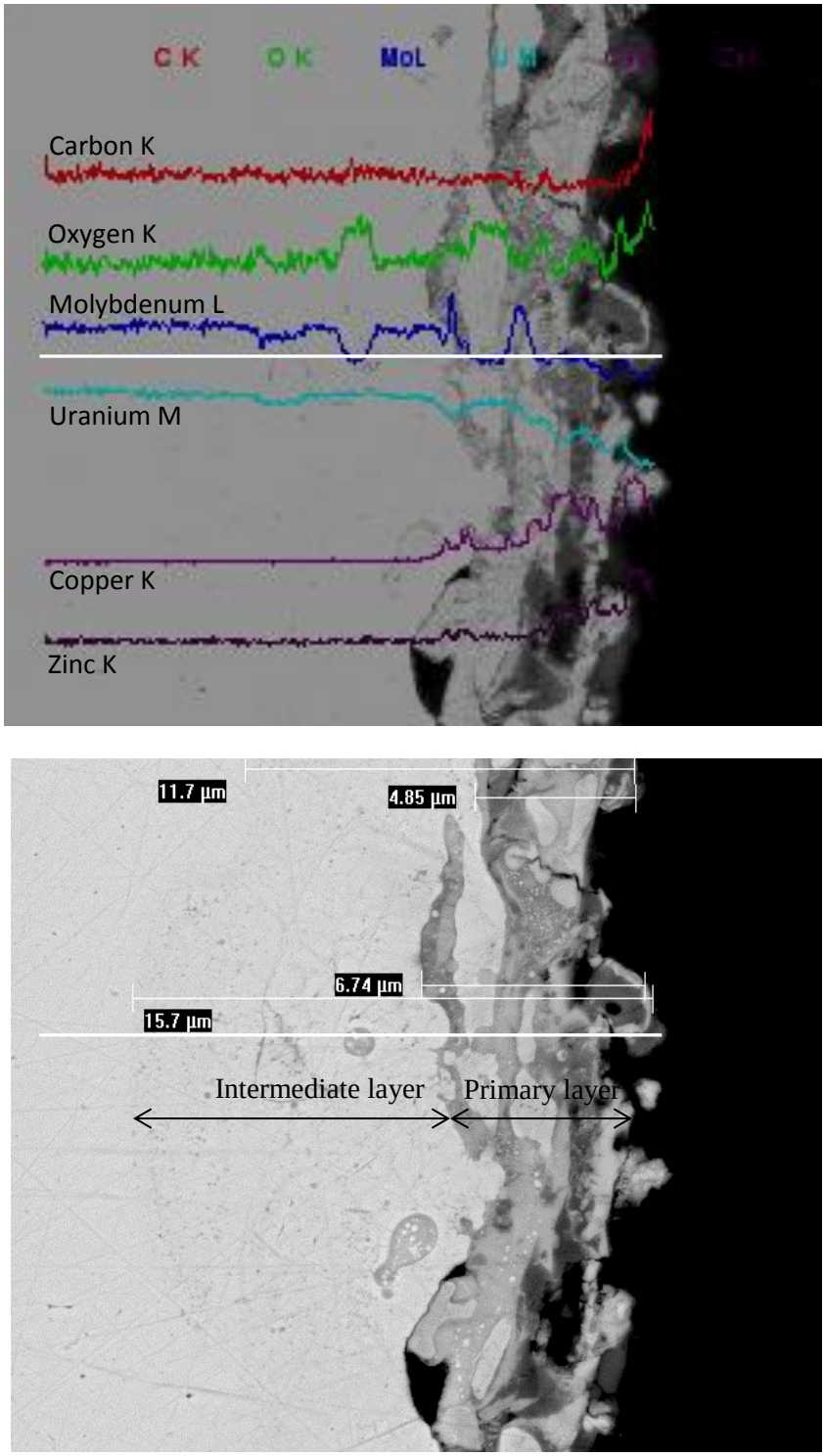

Figure 8. Top: A 19 micron line scan showing elemental distributions through the recast layer. The line scan follows the white line near the center of the image. Colored lines match colored element symbols. Bottom: A reference image with different thicknesses of the recast layer measured.

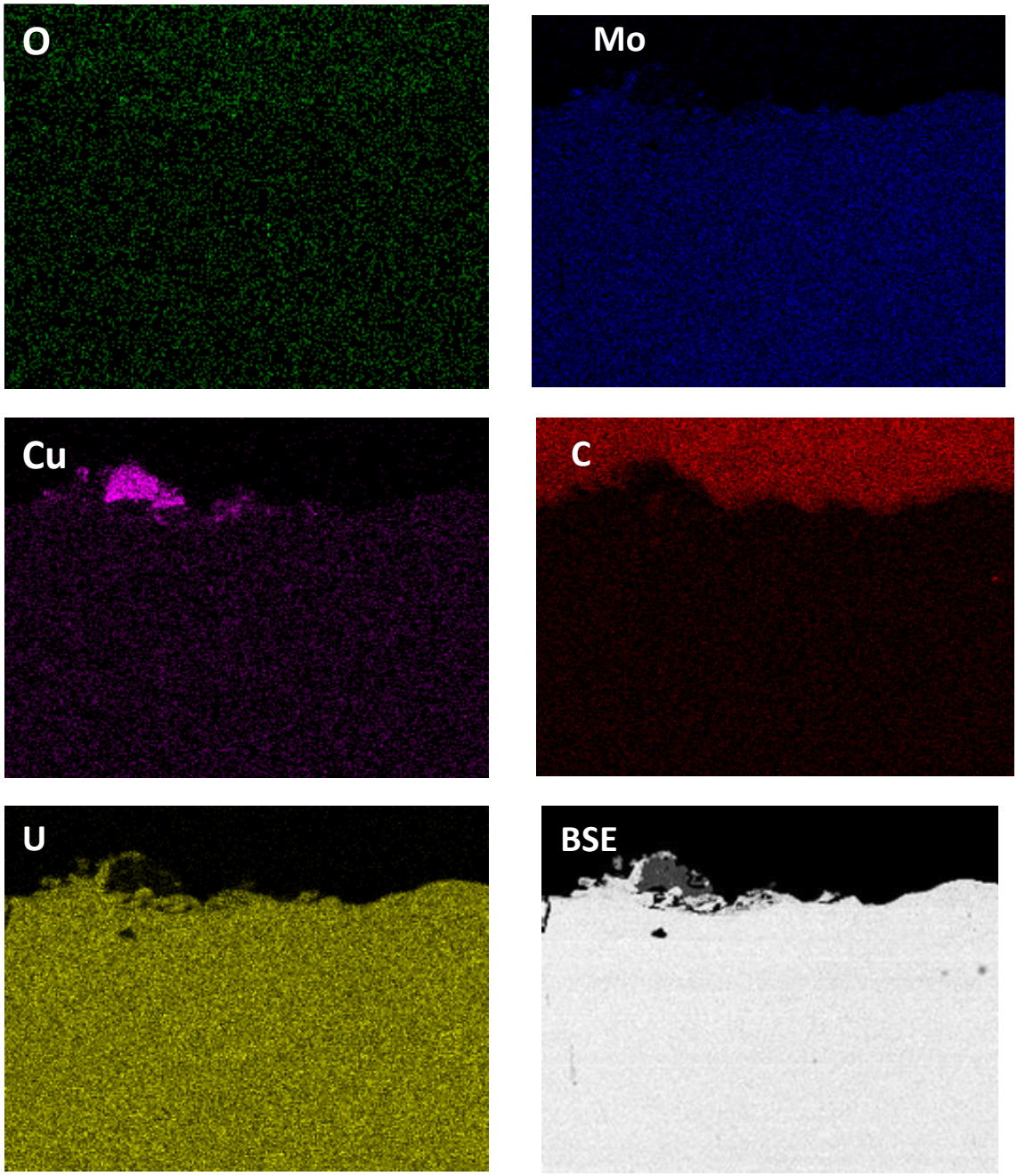

Figure 9. X-ray maps show that the recast contamination layer is discontinuous. When present, it ranges in thickness up to 16 microns and varies in composition in terms of Cu or U being more abundant.

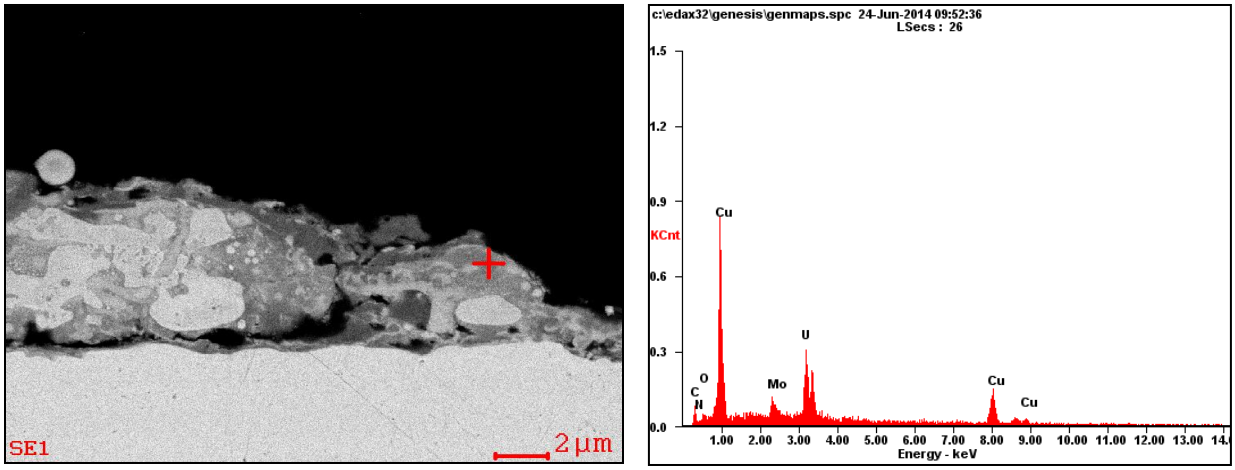

Figure 10. EDS Spectra of recast layer on U-10Mo. Note the presence of Cu peaks from the wire.

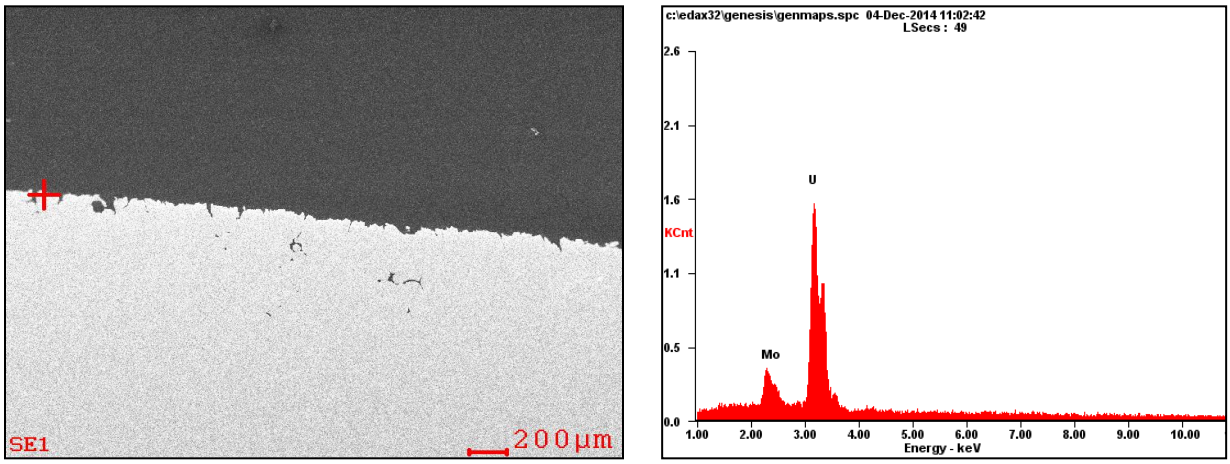

Figure 11. EDS Spectra following cleaning after 20 microns of material are removed from the surface. There are no copper peaks in the spectra.

Graphite Contamination of Exterior Slices

Exterior U-10Mo slices have a surface adjacent to the graphite mold. Typically 0.040" (1 mm) are machined from an exterior face to eliminate any major graphite inclusions and carbon reaction layers, as was the case for this study. Exterior metallography coupons were characterized and the graphite contamination layer was observed to be on the order of a few microns. This layer is shown in Figure 12 along with the corresponding EDS spectra.

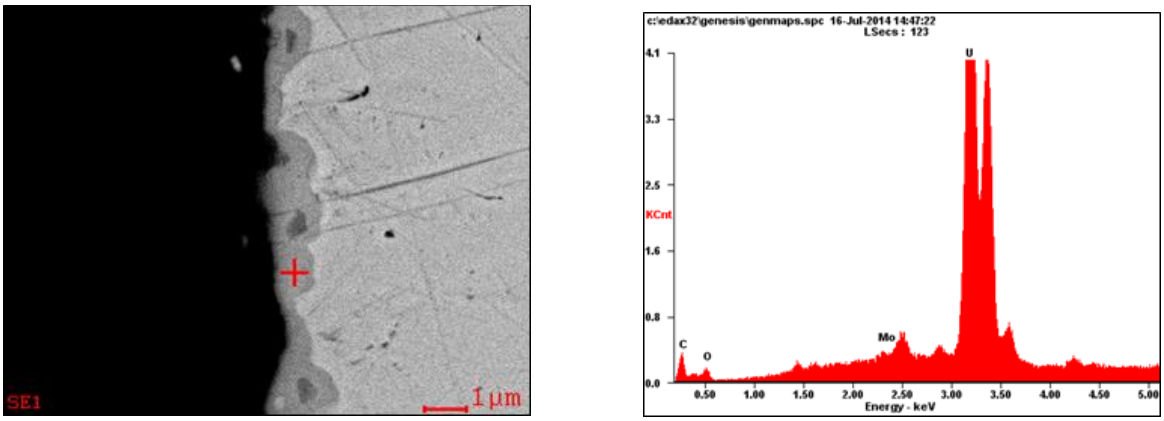

Figure 12. EDS Spectra of contamination layer with graphite crucible.

Homogenization Heat Treatment

In order to reduce or remove chemical segregation, a homogenizing heat treatment is performed. This is conducted at high temperatures to allow for sufficient diffusion of materials. The U-10 Mo coupons were heat treated under vacuum at 1000^{o}C for 4 hours, held at 850^{o}C for one hour, and quenched in oil.

Cleaning, Can Assembly and Welding

The process for fabricating Zr-clad U-10Mo nuclear fuel foils is called pack rolling. This involves enclosing the parts to be welded in a sealed pack which is evacuated under vacuum. The advantages of this process are the atmospheric protection provided for reactive materials such as uranium and zirconium, and that several layers of parts can be welded in one compact assembly. The components for the compact assembly for the interior and exterior U-10Mo slices are shown in Figures 13 and Fig. 14, respectively. The rolling can was fabricated from mild steel plate. The size of the top and bottom covers was 5" x 6" x 0.25" (12.7 cm x 15.2 cm x 0.64 cm). The mild steel plates were thicker than those previously used. A more typical thickness is 0.162" (0.41 cm). An increase in the thickness of the can may affect the heating and reheating time during hot rolling. The outer size of the "picture frame" was 5"x 6" (12.7 cm x 15.2 cm) with an inner cutout of 3.06" x 4.06" (7.7 cm x 10.3 cm) to accommodate the 3" x 4" (7.6 cm x 10.2 cm) coupon. The thickness of the picture frame was 0.135" (0.34 cm), similar to the U-10Mo coupon thickness. The corner of the frame was machined with a 1/8" (0.32 cm) radius. However, the coupon did not fit within the picture frame and a 90^{o} angle corner was later machined with EDM. Two pieces of zirconium foil, per can assembly, with the dimensions of 4.5" x 3.5" x 0.010" (11.4 cm x 8.9 cm x 0.025 cm) were sheared.

Components of the can were cleaned prior to welding of the can. Steel components were cleaned in a Blue Gold bath. Zirconium foils and U-10Mo were cleaned in Blue Gold followed by nitric-2% ammonium bifluoride soak for two minutes. The cleaning operation typically removes approximately 20 grams of material from the U-10Mo coupon. The cleaning operation is summarized in a report by Edwards et al.[2]

The rolling can was assembled with Zr on either side of U-10Mo. The rolling can consists of three layers of steel plate, one of which has a U-10Mo coupon-sized hole cut in the center ("picture frame"). Neolube parting agent is applied by brush between the Zr and the steel can, and the Zr is tack welded to the outer steel pieces.

The rolling can was Gas Tungsten Arc (GTA) welded in an argon (<20 ppm O_2) atmosphere to seal the contents. The welded can is shown in Figure 15.

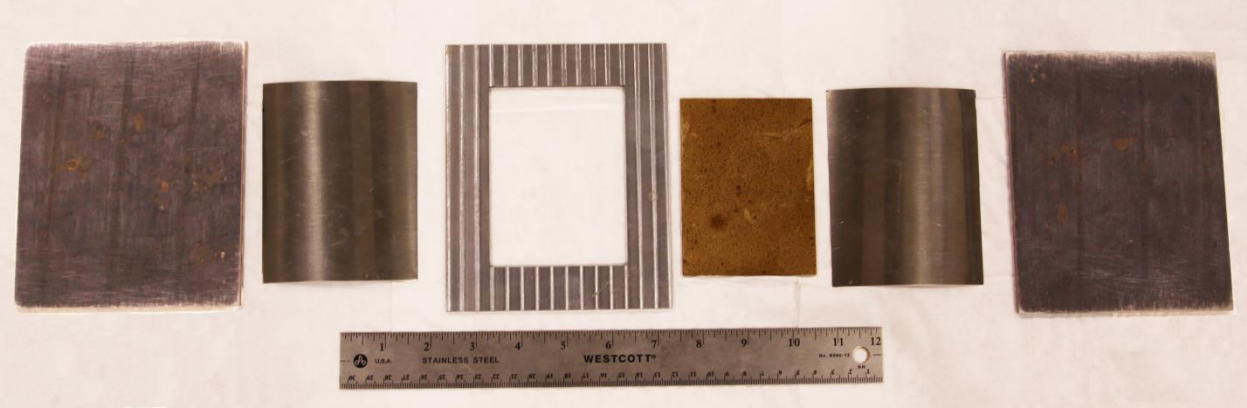

Figure 13. Can components for interior slice coupon. From left to right: mild steel cover, Zr sheet, mild steel picture frame, U-10Mo coupon, Zr sheet, mild steel cover.

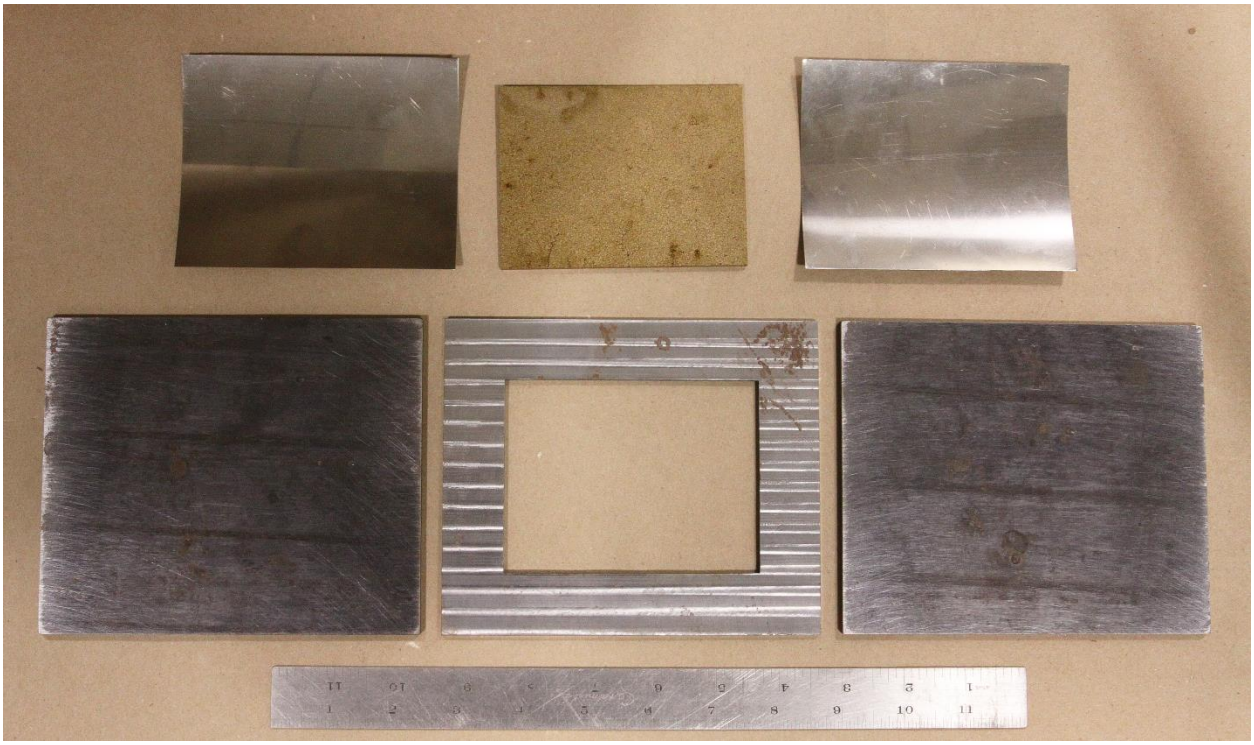

Figure 14. Can components for exterior slice coupon. Top row from left to right: Zr sheet, U-10 Mo coupon, Zr sheet. Bottom row left to right: mild steel cover, mild steel picture frame, mild steel cover.

Figure 15. Welded mild steel can for interior U-10Mo coupon.

Hot Rolling

Hot rolling involves work above the recrystallization temperature of the workpiece. Canned coupons were heated in a 680^{o}C air furnace for 30 minutes followed by rolling in approximately 10% reductions per pass from the initial 0.635 inches (16 mm) to a final can thickness of 0.100 inches (2.5 mm). The assembly was reheated 5 minutes between each pass. The mild steel can was annealed for 30 minutes in a 680^{o}C air furnace. The mild steel can is then removed using a foot shear to prepare for cold rolling, shown in Figure 16. The thickness of the hot rolled foil was 0.021" (0.53 mm) and 0.019" (0.48 mm) for the interior and exterior slices, respectively. Macros of a piece cut from the hot rolled interior and exterior foils are shown in Figures 17 and Fig. 18, respectively. Differences in the surface roughness are more apparent upon closer examination of the interior and exterior foils shown in Figures 19 and Fig. 20, respectively. Removing the can from the exterior foil proved difficult as the Zr layer did not bond to the U-10Mo but was peeled away upon removal of the mild steel can. This lack of bonding may have been related to cracking within the exterior U-10Mo coupon. However, cracking was noted in the interior U-10Mo coupon and the Zr bonded to the U-10Mo substrate.

Figure 16. Left: interior coupon following hot rolling with mild steel can removed. Right: Close up of hot rolled interior slice Zr-clad U-10Mo.

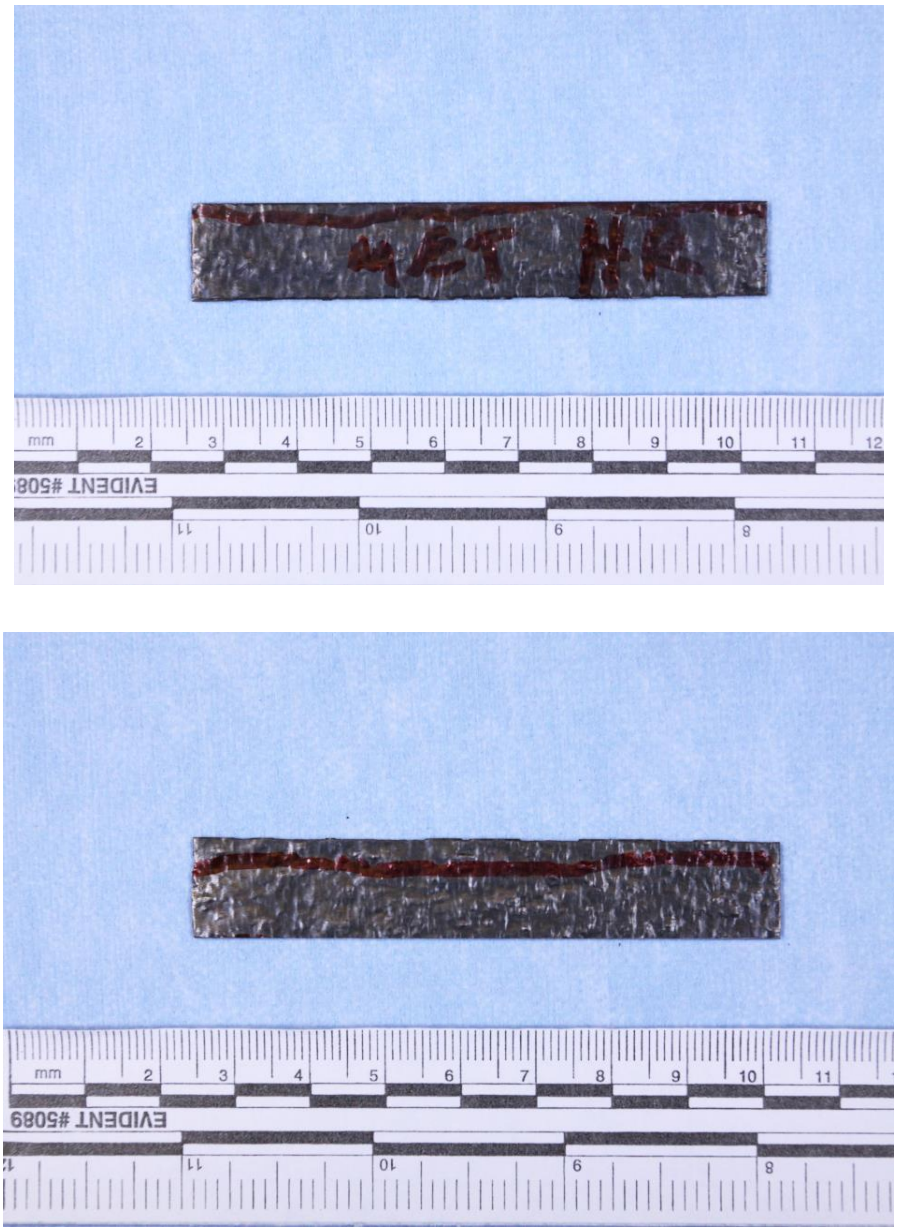

Figure 17. Macro of sample of both sides of hot rolled Zr-clad U-10Mo foil from interior slice coupon.

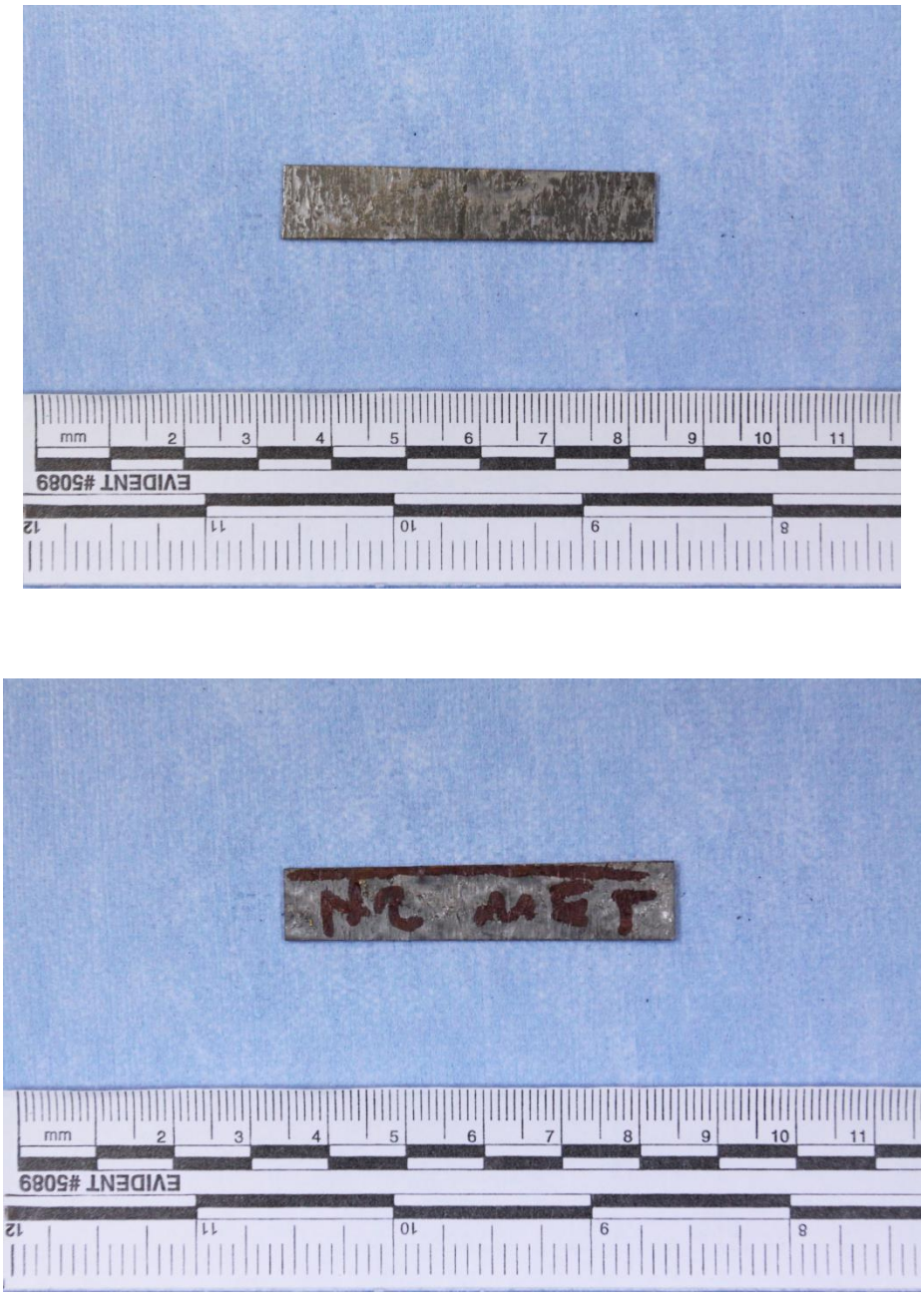

Figure 18. Macro of sample of both sides of hot rolled U-10Mo foil from exterior slice coupon.

Figure 19. Front and back sides of hot rolled interior slice Zr-clad U-10Mo coupon showing surface roughness.

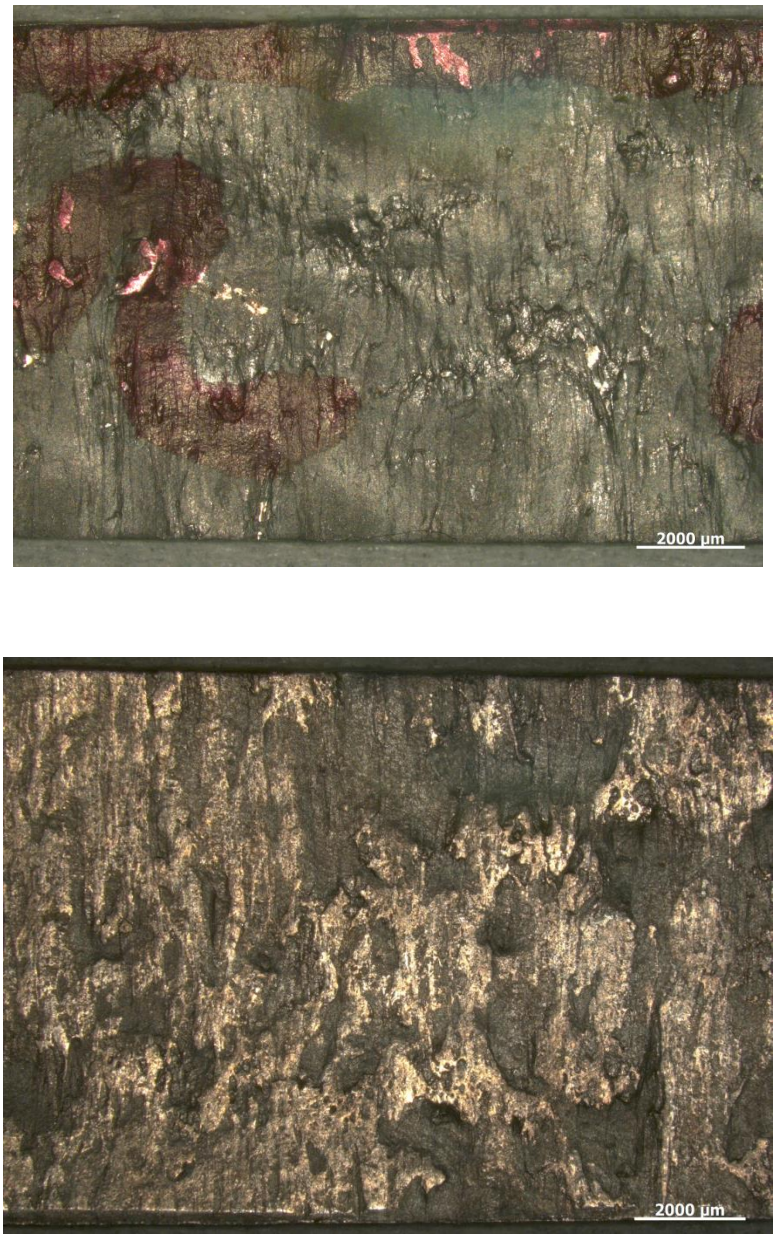

Figure 20. Front and back sides of hot rolled exterior slice U-10Mo coupon showing surface roughness. Most of the Zr cladding adhered to the steel can.

Cold Rolling

Cold rolling is done at temperatures below the recrystallization temperature which increases strength by strain hardening. It also improves the homogeneity, uniformity and surface finish of the foil. The coupons were rolled to a final thickness of 0.015" (0.38 mm) and 0.011" (0.28 mm) for the interior and exterior EDM slice, respectively. This requires typically 8-10 passes. The cold rolled interior and exterior slice foils are shown in Figures 21 and Fig. 22, respectively. Again, the difference in the appearance of the foils is from the lack of sufficient bonding of the Zr with the exterior slice U-10Mo coupon. Sections of the interior and exterior slice foils are

shown in Figures 23 and Fig. 24, respectively. A closer examination of the foil surface is displayed in Figures 25 and Fig. 26, respectively. The surface roughness of the Zr-clad interior slice coupon appears different from top to bottom. Cracking is noted in the images of the exterior slice coupon.

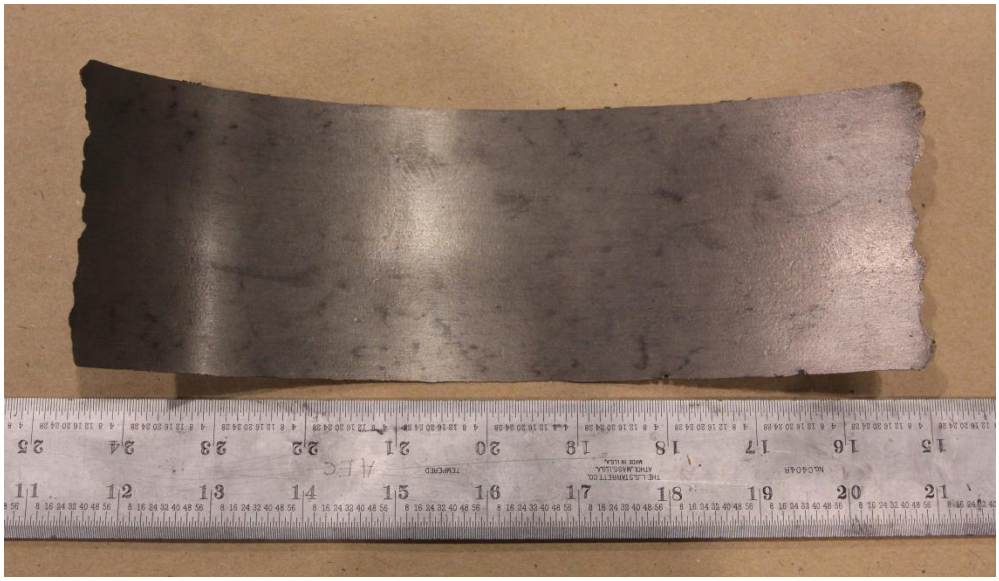

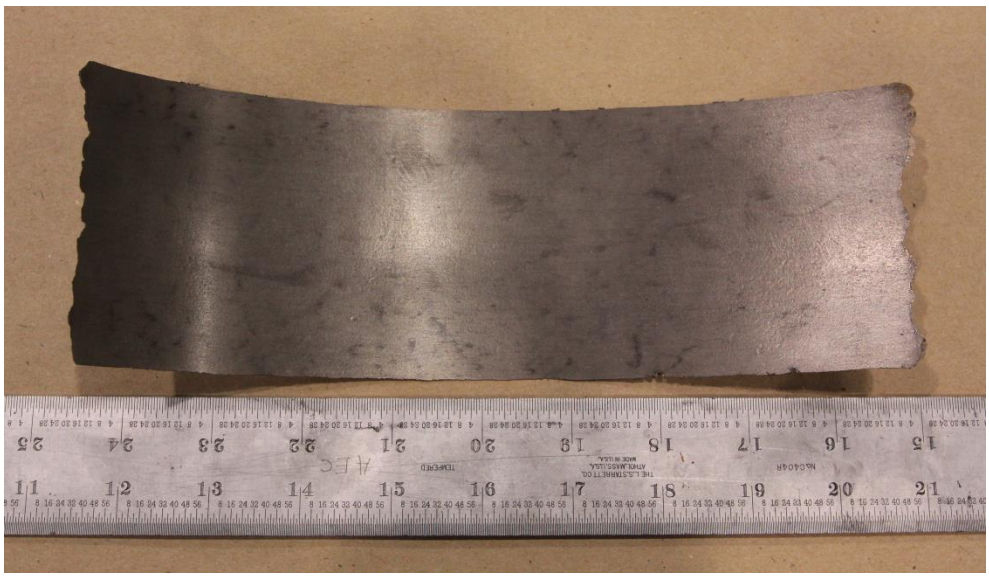

Figure 21. Front and back surface of cold rolled interior slice Zr clad U-10Mo coupon.

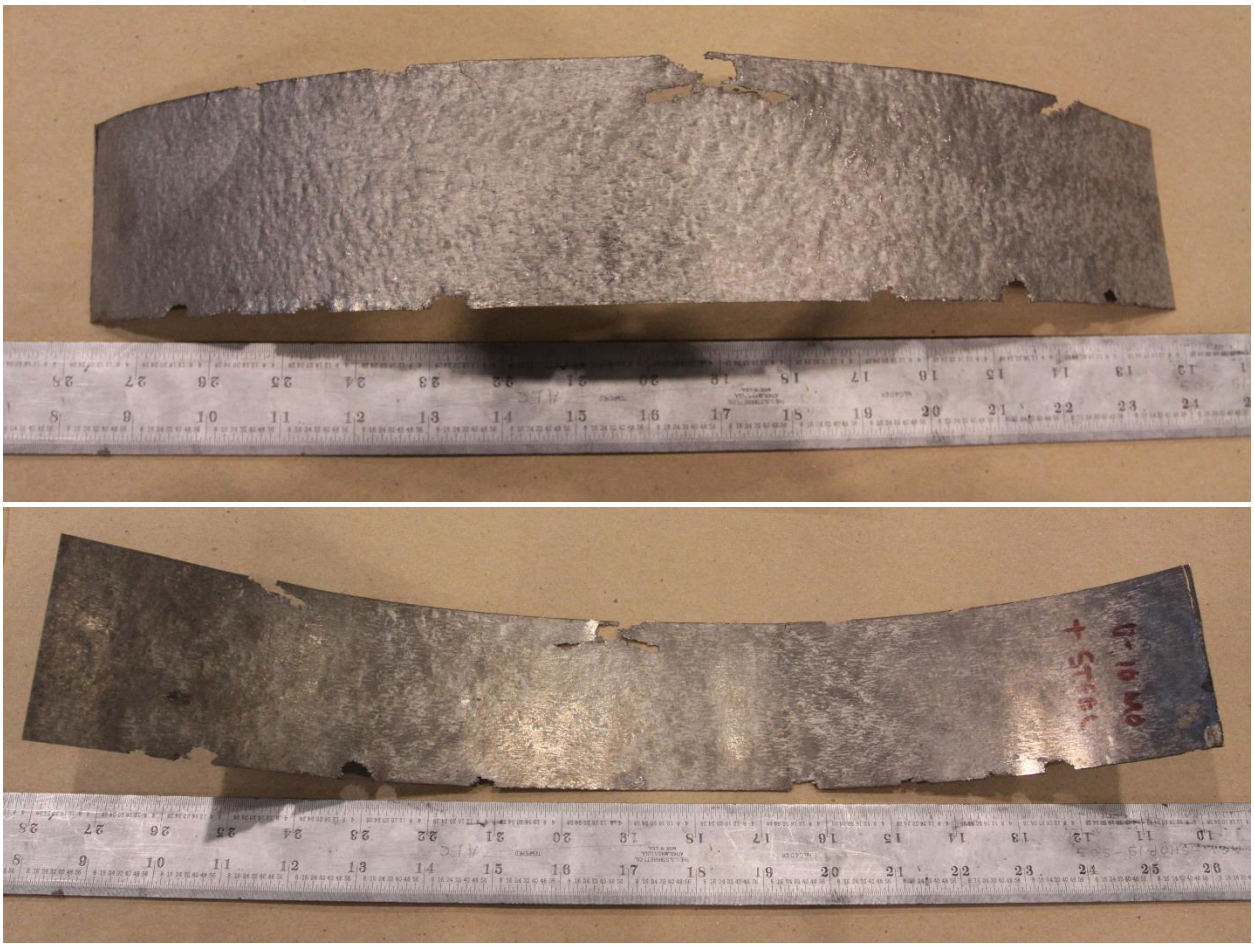

Figure 22. Front and back surface of cold rolled exterior slice U-10Mo coupon. Most of Zr cladding peeled from surface upon steel can removal.

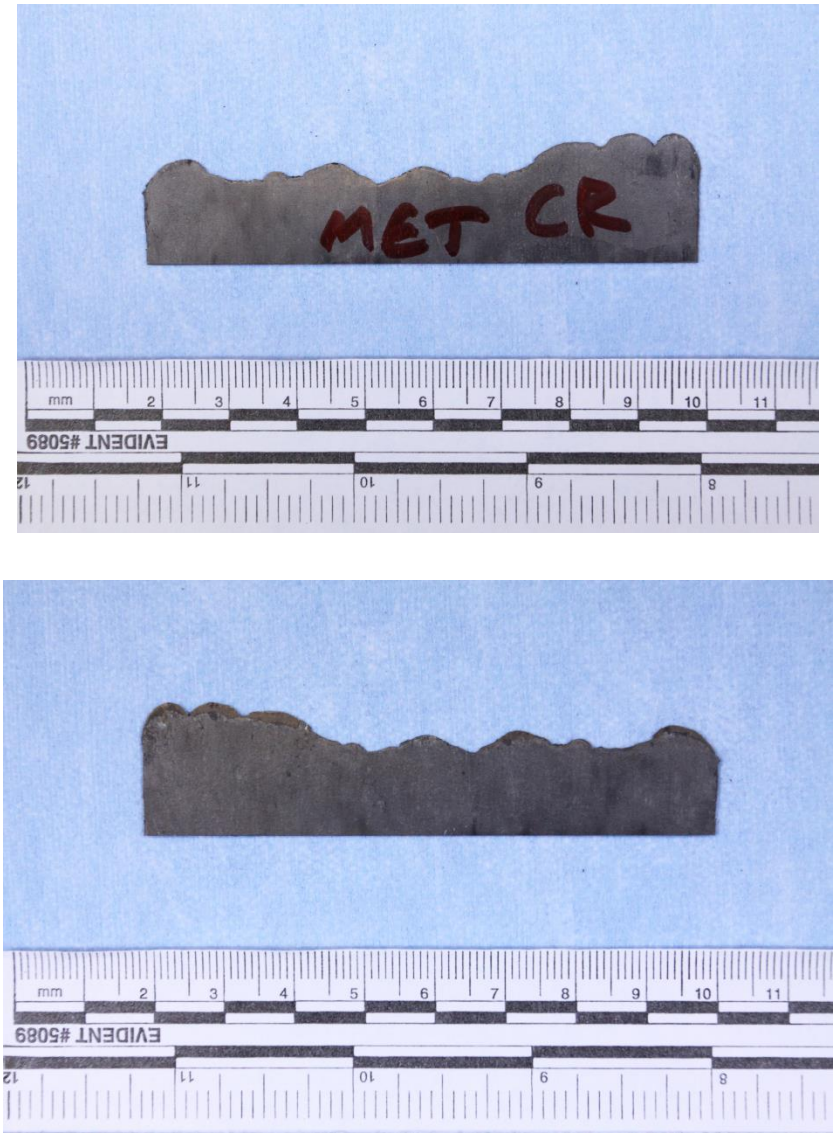

Figure 23. Both sides of section of cold rolled Zr- clad U-10Mo Foil from interior slice coupon.

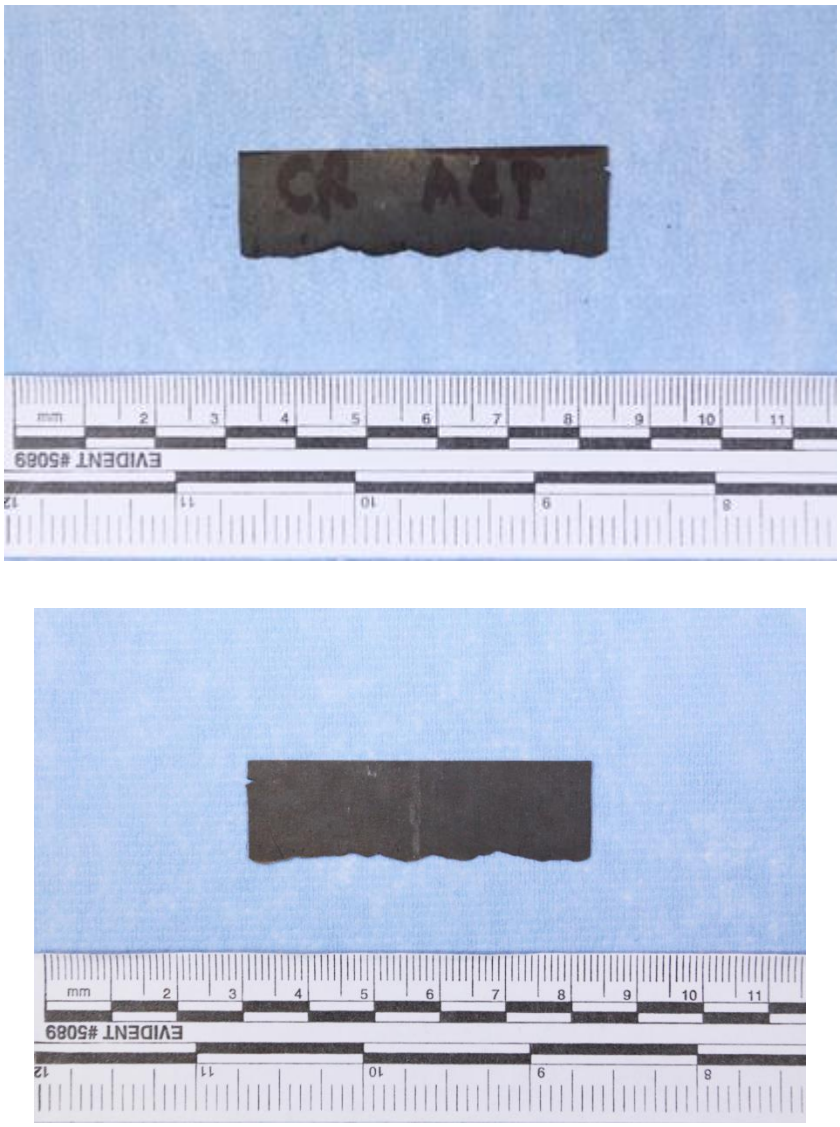

Figure 24. Both sides of section of cold rolled U-10Mo foil from exterior slice coupon. Zr cladding was removed upon separation of steel rolling can following hot rolling.

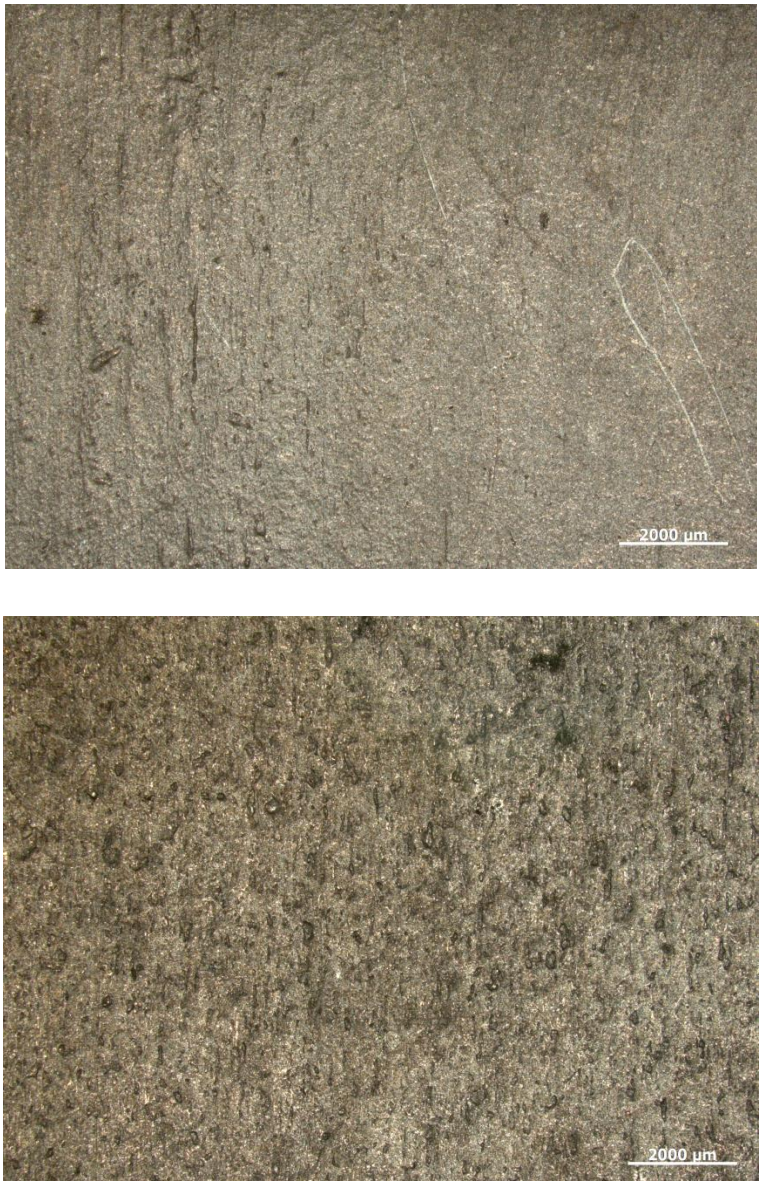

Figure 25. Front and back surface of cold rolled interior slice Zr-clad U-10Mo coupon.

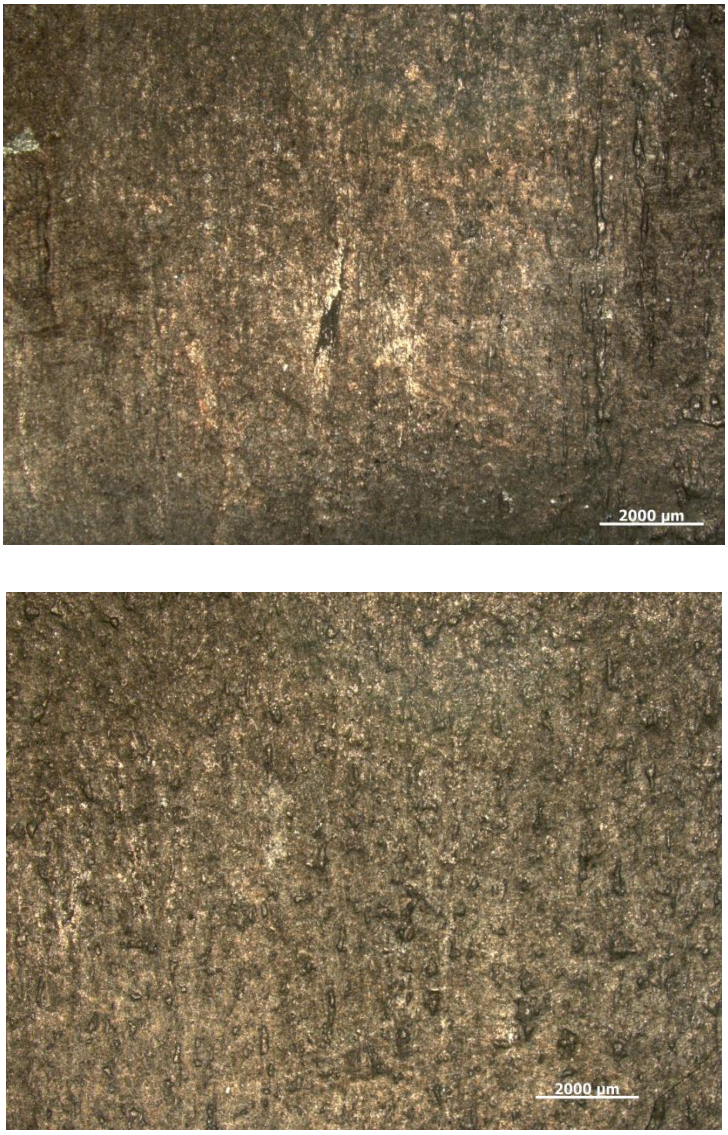

Figure 26. Front and back surface of cold rolled exterior slice U-10Mo coupon. Zr cladding peeled from surface after hot rolling following removal of mild steel can.

Metallographic Preparation

Grinding of metallographic samples was done on the following SiC grits: 120, 320, 600, and 800. Samples were then polished according to the procedure in Table 3. MOL cloth is a woven wool medium/soft cloth. NAP is a soft, very short napped synthetic cloth used for final polishing. Metallographic preparation was challenging due to the different properties of the dissimilar metals. To get the optimal preparation, a greater force was used for a longer period of time than used for the initial preparation. Images were taken on a Zeiss AxioObserver microscope with a Zeiss AxioCam HRc digital camera. Zeiss AxioVision software was used for image capture and microscope control.

Table 3. Metallographic preparation for polishing U-10Mo.

Suspension	Polishing Time	Force	Polishing Cloth	Platen Speed	Head Speed	Head Rotation
3μm	4 minutes	40 N	MOL	120 RPM	100 RPM	Counter-rotation
3μm	3 min, 30 sec	15 N	MOL	150 RPM	150 RPM	Co-rotation
1 μm	4 minutes	40 N	MOL	120 RPM	100 RPM	Counter-rotation
1 μm	3 minutes	15 N	MOL	150 RPM	150 RPM	Co-rotation
Colloidal Silica	2 min, 30 sec	15 N	NAP	150 RPM	150 RPM	Co-rotation

Characterization of Interior Slice Zr clad- U-10Mo foils

Micrographs of the hot rolled Zr-clad U-10Mo interior slice are shown in Figures 27-30 with a Zr cladding thickness up to 100 microns and an average thickness of approximately 55-60 microns. Some micro-cracking was noted at the Zr/U-10Mo interface in the longitudinal section in Figure 28. In the transverse section of Figure 28, the Zr/U-10Mo interface consists of overlapping layers as opposed to the straight interface usually observed. The grain structure of the zirconium appears equiaxed with a grain size of about 40 microns and is shown in Figure 30. The grain structure of the U-10Mo fuel is exhibited in Figures 31-33. The structure consists of equiaxed grains 5-50 microns in size with some highly elongated grains with lengths as large as a few hundreds of microns. Interaction layers develop at the Zr/U-10Mo interface as a result of high temperature exposures during processing. Differential interference contrast (DIC) images at the Zr/U-10Mo interface are shown in Figure 34. A eutectic-type microstructure is observed in the U-10Mo at the interface and has been described previously as α-U lamellae in γ-U-Mo.[3] Micro-cracking was prevalent at the hot-rolled Zr-clad U-10Mo interface, shown in Figure 35. A thin film intermediate reaction layer was also observed at the interface. This layer was on the order of one micron in thickness making it difficult to analyze using EDS. There was also a granular reaction layer with the appearance of submicron individual grains. In order to properly identify these reaction layers, transmission electron microscopy (TEM) at the interface should be pursued.

Micrographs of the cold rolled Zr-clad U-10Mo interior slice are shown in Figures 36-37. The Zr cladding thickness measured up to 63 microns with an average of 20-30 microns. Less micro-cracking (50%) was observed in the cold rolled foils at the Zr-clad/U-10Mo interface, most notably in the longitudinal section in Figure 37. The microstructure of the zirconium is shown in Figure 38. Grains appear deformed as opposed to equiaxed, as seen in the hot rolled foil. Some deformation twins were observed in the zirconium. Figure 39 shows the U-10Mo structure which is composed of deformed grains with a bimodal distribution. Banding is noted in Figure 40. Carbide stringers in the U-10Mo have been observed to align with these bands,[4] but carbides appear to be randomly distributed in this study. Banding is associated with variation in

Mo composition.[4] Figure 41 shows a SEM micrograph of the Zr/U-10Mo interface following cold rolling. Upon closer examination in Figure 42, four reaction layers between the zirconium and U-10Mo are evident. The scale of the reaction product was below the resolution for EDS analysis and requires TEM for confirmation of reaction product composition. Perez et al. noted the following phases at the Zr/U-10Mo interface, using TEM: δ-UZr_2 (a 2 micron thick continuous reaction layer in contact with Zr barrier plate), γ-U (bcc) stabilized with Zr (next to δ-UZr_2), Mo_2Zr (continuous non-planar layer up to 250 nm thick between Zr and U-10Mo), and α-U lamellae with matrix of γ-U10Mo (region near U-10Mo).[3] The U-10Mo was γ-U (bcc) phase while α-U has an orthorhombic structure. Observations in literature of interaction layers at the Zr/U-10Mo interface are summarized in Table 4. Micro-cracking was frequently observed at the Zr/U-10Mo interface with the formation of reaction phases, as shown in the longitudinal section in Figure 37. The cracking has been attributed to a volume change between precipitates and the surrounding matrix.[4]

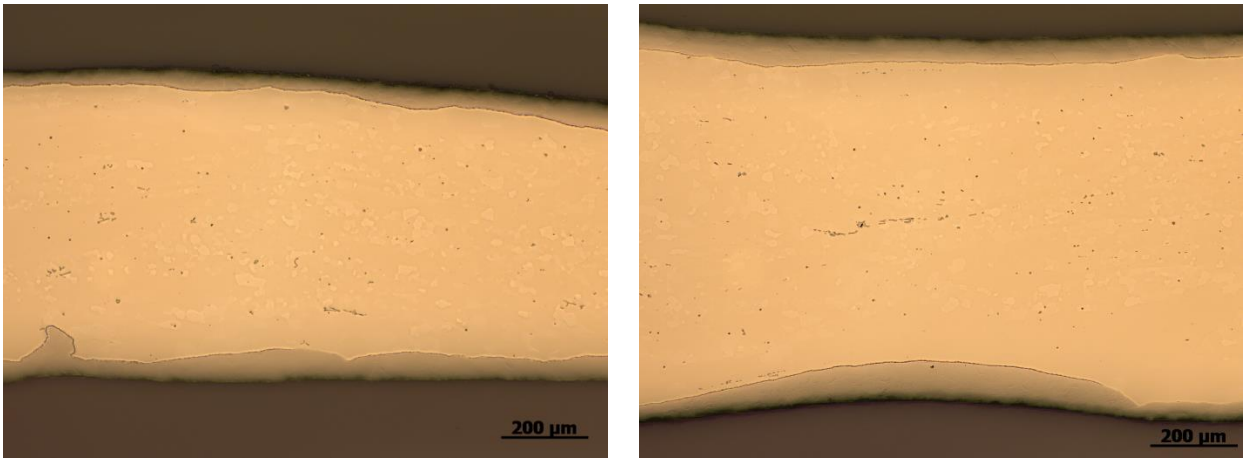

Figure 27. Metallographic sections of hot rolled interior slice Zr clad U-10Mo foil. The longitudinal section is on the right and transverse section is on the left.

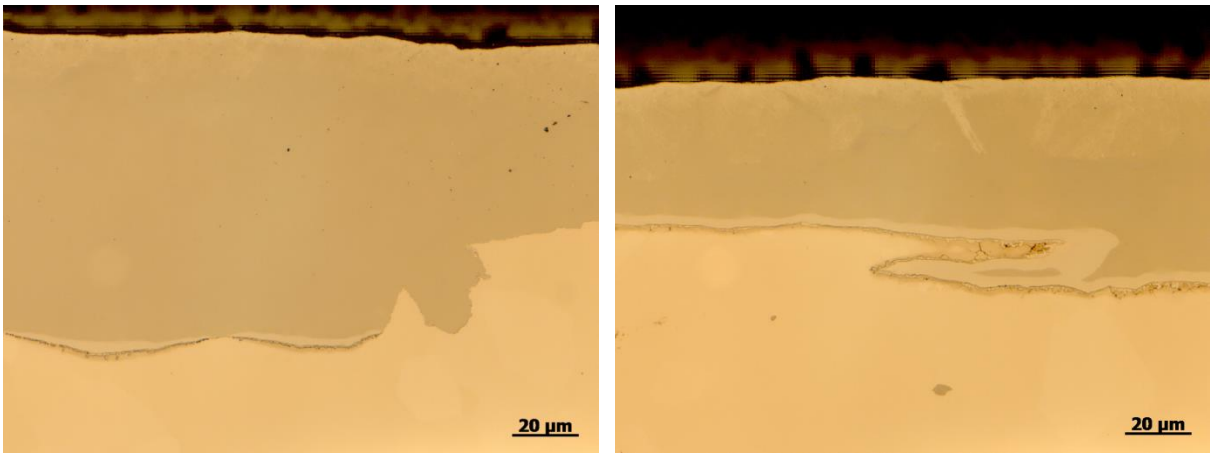

Figure 28. Metallographic sections of hot rolled interior slice Zr clad U-10Mo foil. The longitudinal section is on the left and the transverse section is on the right.

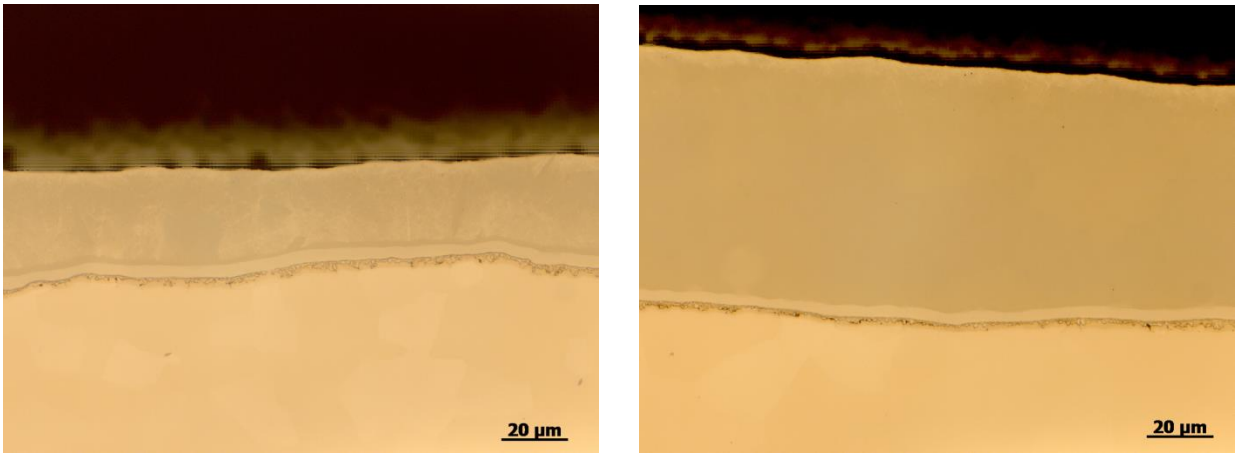

Figure 29. Metallographic cross sections of hot rolled interior slice Zr clad U-10Mo foil. The longitudinal section is on the left and the transverse section is on the right.

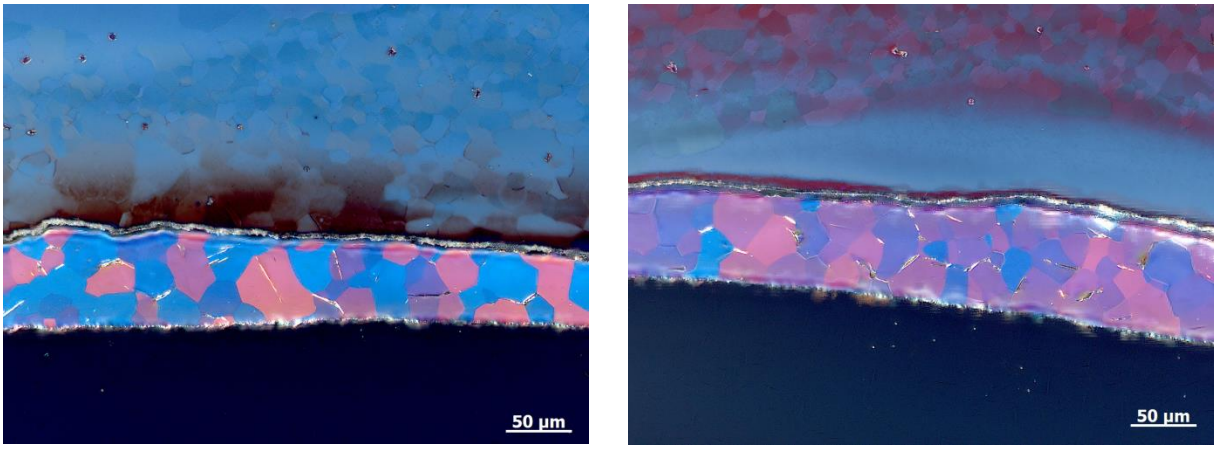

Figure 30. Polarized light images of hot rolled Zr-clad U-10Mo showing Zr microstructure: longitudinal section on left, transverse section on right.

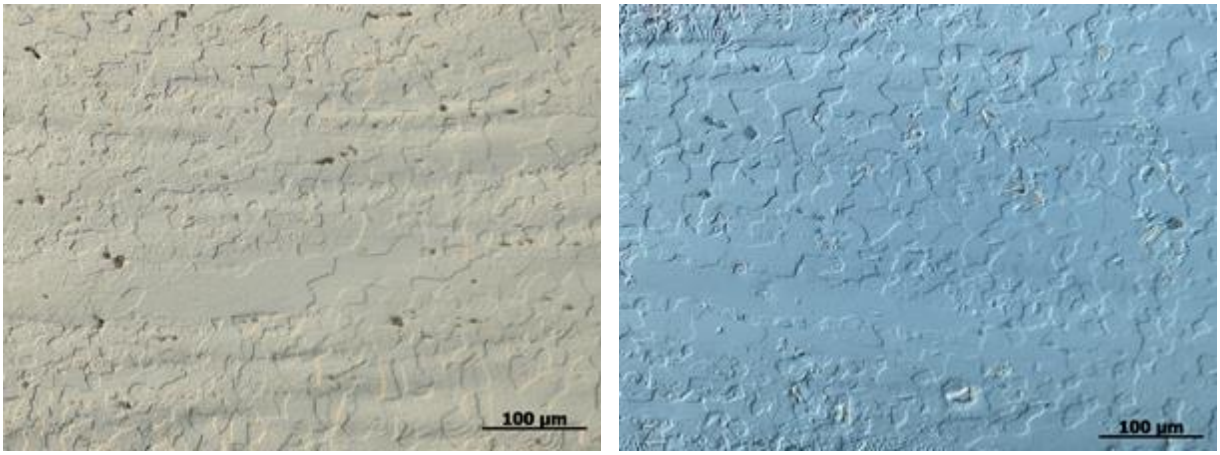

Figure 31. U-10Mo grain structure of hot rolled Zr-clad interior EDM slice coupon: longitudinal section (left), transverse section (right). (DIC)

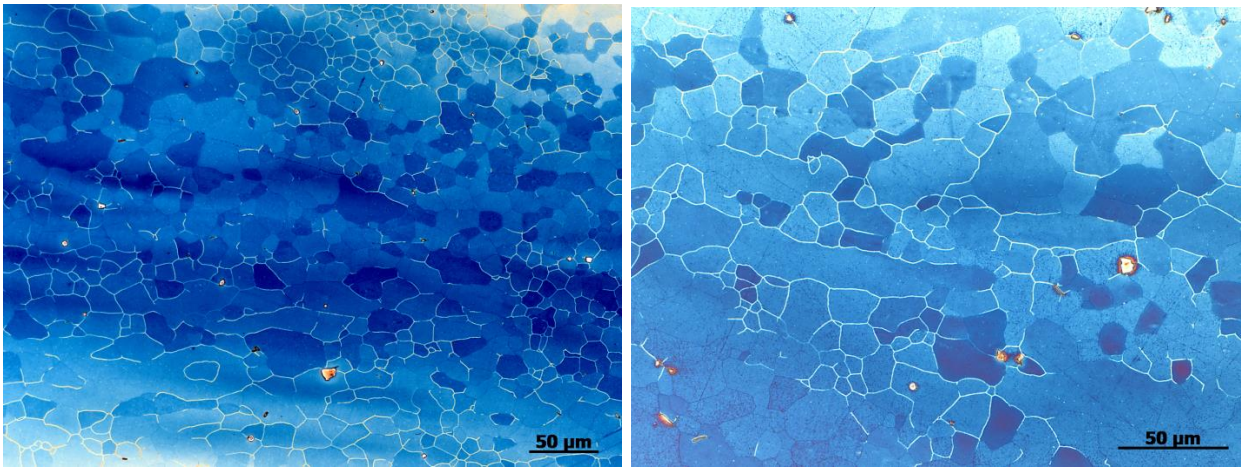

Figure 32. U-10Mo grain structure of hot rolled Zr-clad interior EDM slice coupon: longitudinal section (left), transverse section (right). (Bright field)

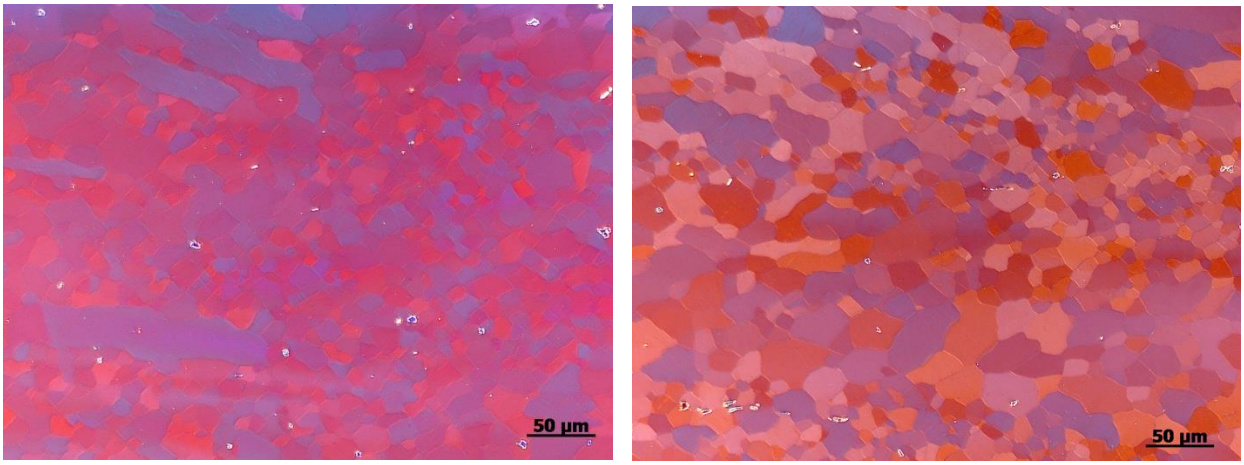

Figure 33. U-10Mo grain structure of hot rolled Zr-clad interior EDM slice coupon: longitudinal section (left), transverse section (right). (Polarized Light)

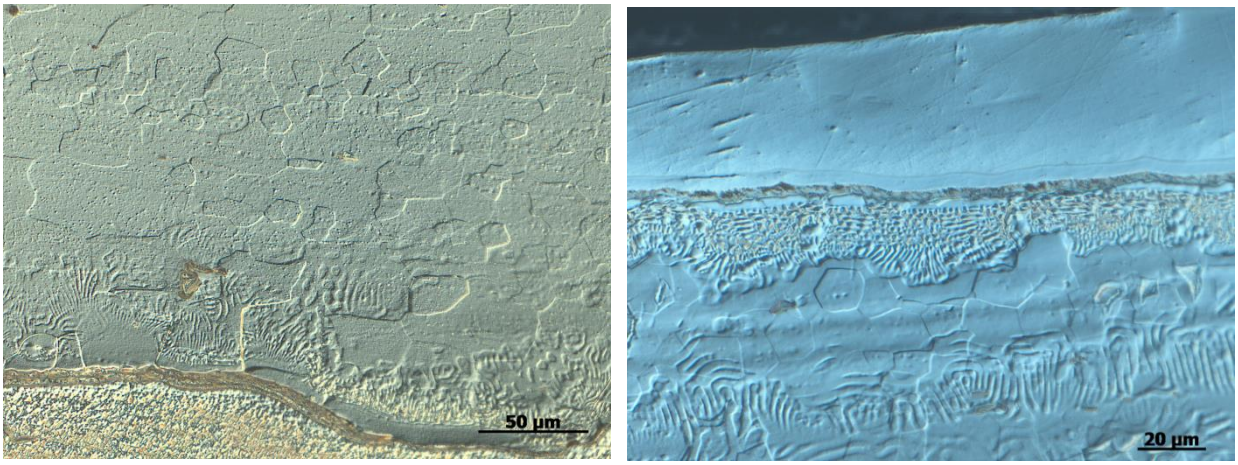

Figure 34. Differential interference contrast (DIC) images of Zr/U-10Mo interface following hot rolling showing eutectic structure. The longitudinal section is on the left and transverse section is on the right.

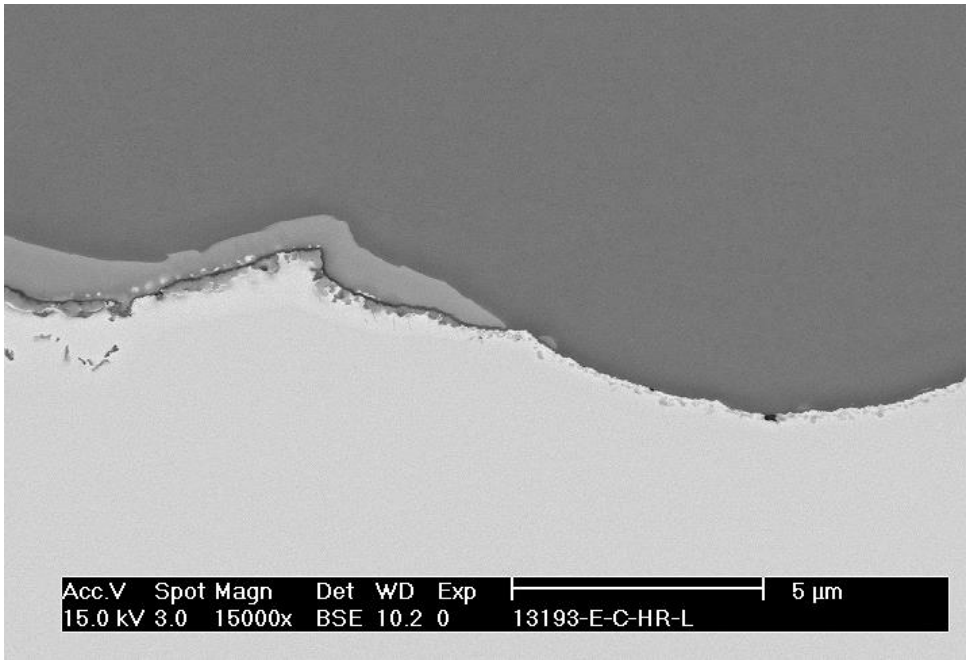

Figure 35. Micro-cracking noted between the thin film reaction layer adjacent to the Zr and the granular reaction layer adjacent to the uranium in hot rolled Zr-clad U-10Mo (interior slice).

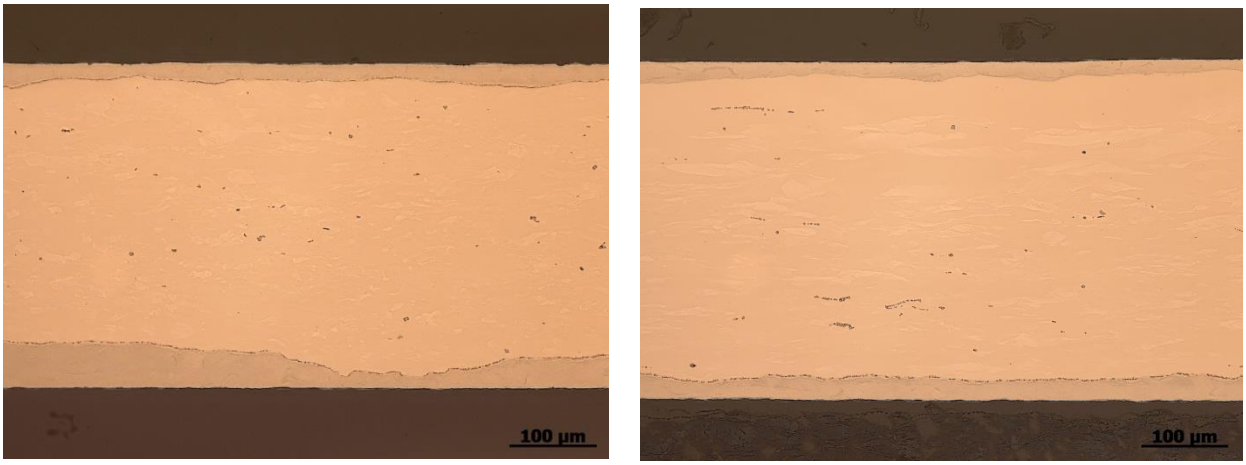

Figure 36. Metallographic cross-sections of cold rolled interior slice Zr clad U-10Mo foil. The longitudinal section is on the left and the transverse section is on the right.

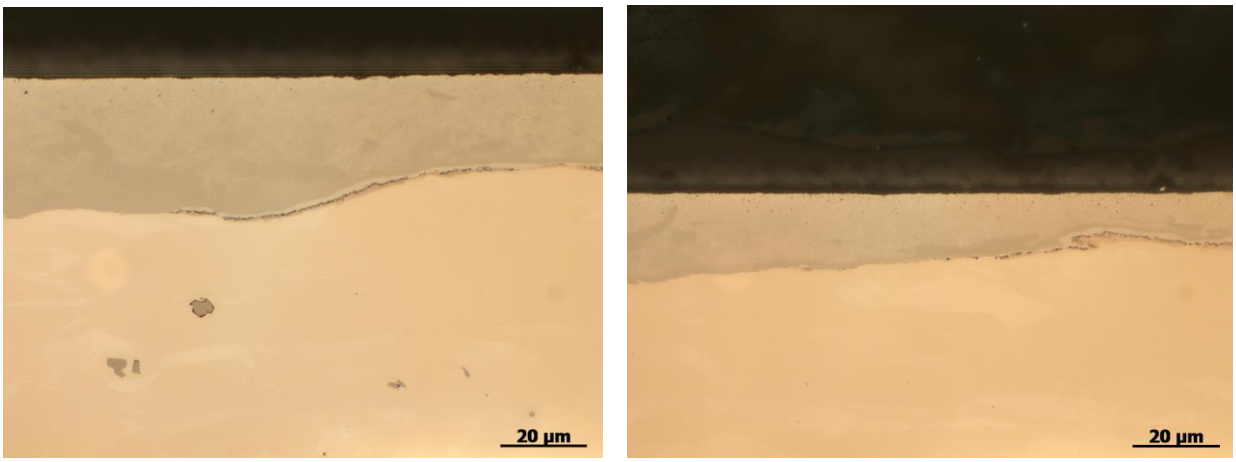

Figure 37. High magnification metallographic images of cross-section of cold rolled interior slice. Longitudinal section is on the left and the transverse section is on the right. Cracking is noted at the interface between the Zr and the U-10Mo.

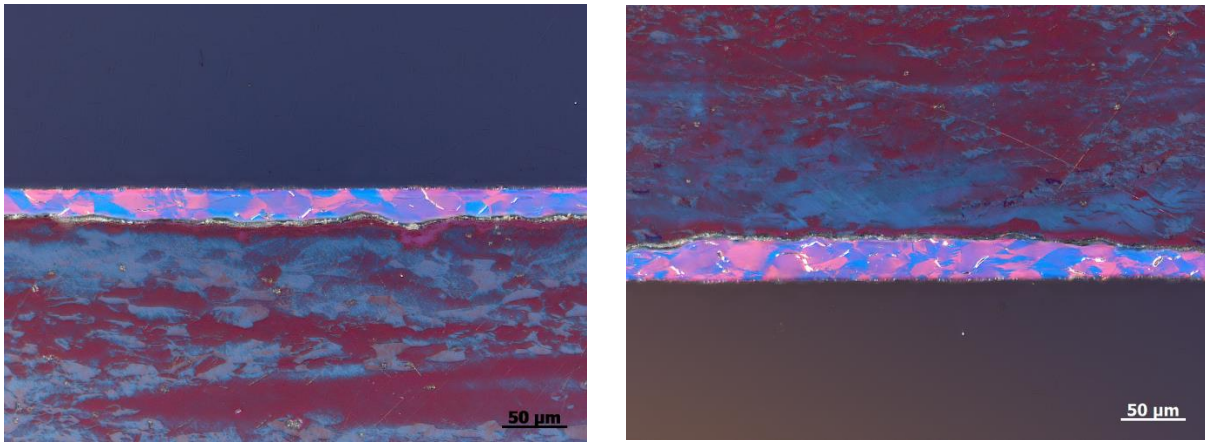

Figure 38. Polarized light image showing grain structure of zirconium in cold rolled Zr/U-10Mo coupon. Longitudinal section is on the left and transverse section is on the right.

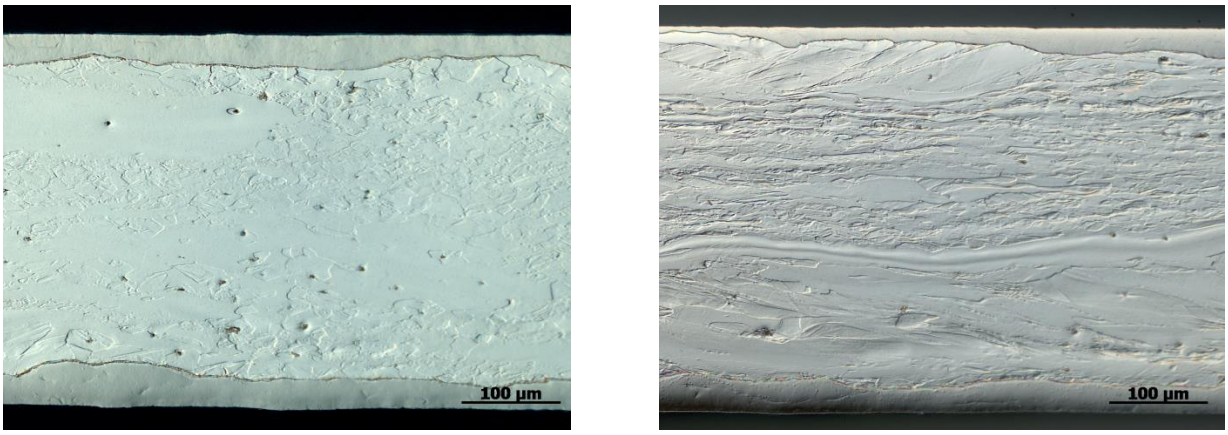

Figure 39. Differential interference contrast images of cold rolled interior slice Zr-clad U-10Mo coupon. Longitudinal section is on the left and transverse section is on the right.

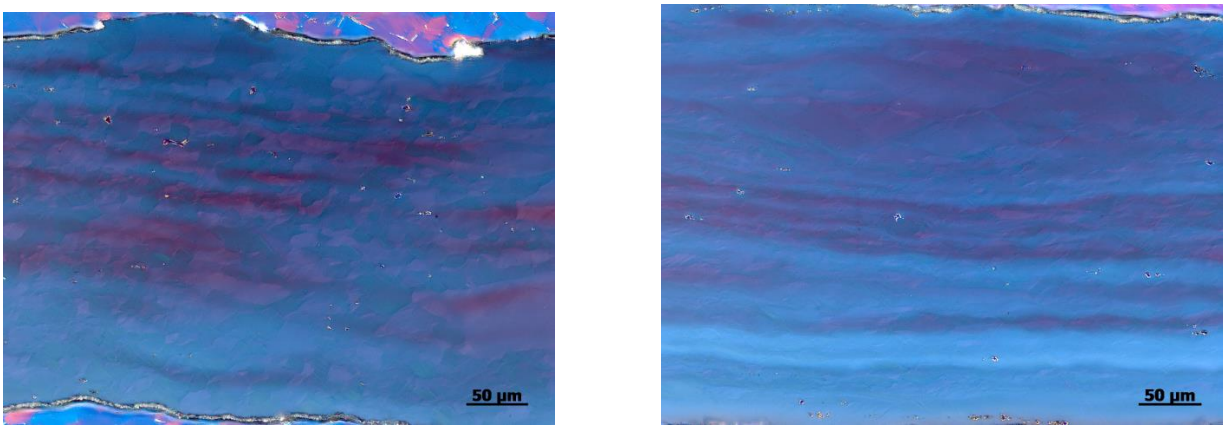

Figure 40. Polarized light images of cold rolled interior slice U-10Mo showing banding. Longitudinal section is on the left and the transverse section is on the right.

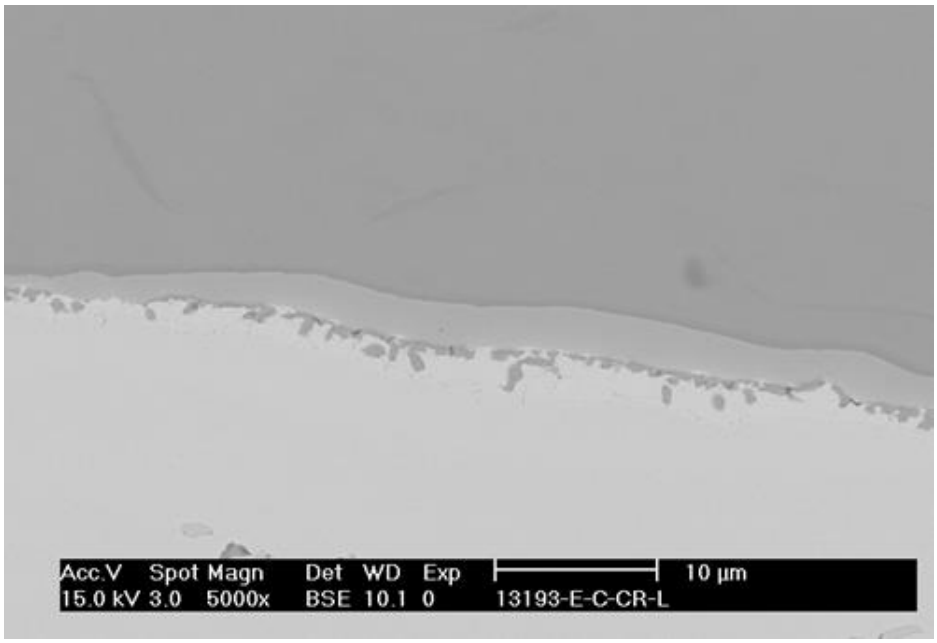

Figure 41. Cold rolled interior slice showing interface between Zr and U-10Mo.

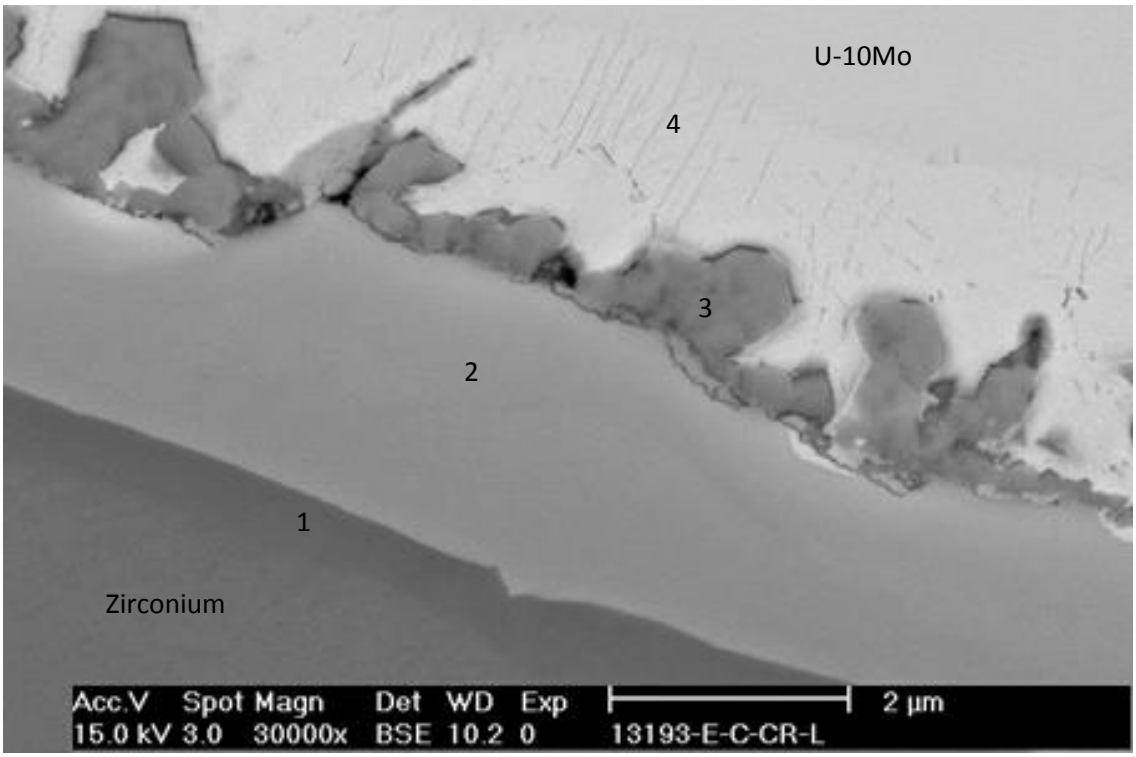

Figure 42. Cold rolled interior slice showing interface between Zr and U-10Mo.

Table 4. Literature Comparison of Grain Size and Zr thickness

Foil ID	U-Mo grain size (μm)	Max. Aspect Ratio	Zr Grain Size Range (μm)	Zr Min. Thickness (μm)	Zr Max. Thickness (μm)	Source	Reference
R9HT-C1 (Trans.)	5-300	15	5-30	21	37	Y-12	4
R9HT-C2 (Long.)	5-500	30	5-30	15	34	Y-12	4
R9HW-1 (Trans.)	5-100	8	5-50	13	28	Y-12	4
R9HW-2 (Long.)	5-300	30	5-50	15	33	Y-12	4
R1X6-A1 (Trans.)	10-250	15	15-100	20	37	LANL	4
R1X6-A2 (Long.)	3-150	15	15-100	7	23	LANL	4
R1X4-1 (Trans.)	5-300	15	15-100	6.5	30	LANL	4
R1X4-2 (Long.)	5-300	15	15-100	6.5	30	LANL	4
EDM-Int. (Trans.)	5->200	>15	5-70	4.2	44	LANL	
EDM-Int. (Long.)	5->300	>15	5-55	6.3	63	LANL	
EDM-Ext. (Trans.)	5->200	>20	NA	NA	NA	LANL	
EDM-Ext. (Long.)	5->500	>8	NA	NA	NA	LANL	
HIP52-1	11-14 avg.	NM	7-100	32	47	INL	5, 6
FB126	15-19 avg.	NM	5-38	14	54	INL	6
PNNL-24135 (irradiated)	NM	NM	NM	24-26 avg.	35-39 avg.	INL	7

NA-not applicable, NM-not measured

Table 5. Literature survey of interfacial layer characterization between Zr and U-10Mo.

Reference	Description	Interfacial Layer (P) = porosity, (C) = cracking, **(U)** = uniform	Thickness	Reference Image	Reference Number
LA-UR-12-00323	Plasma sprayed Zr on U	L1: Zr grains	44 nm	7	8
		L2: UO_2 grains	24 nm	7	8
PNNL-21990	Roll bonded LANL Foil ID 3G60-CK-R1X4	L1: Zr w/minor U **(U)**	1.2 μm	3-15	4
		L2: Zr w/ higher U (δ-UZr_2)	0.3 μm, particles 15-50 nm in size	3-15	4
		L3: Mo_2Zr (C, P)	1.9 μm	3-15	4
		L4: mostly U, few % Zr, Mo, O (resembles popcorn)	0.5 μm	3-15	4
PNNL-21990	Roll bonded Y-12 Foil ID 3E67L R9HW	L1: Zr-rich, similar to R1X4 **(U)**	1.4 μm	4-10	4
		L2: no speckled appearance, platelets of δ-UZr_2	0.5 μm	4-10	4
		L3: Mo_2Zr (blocky ppt.)	0.5 μm	4-10	4
		L4: Mo rich phase oriented phase + lighter phase	0-1.5 μm max.	4-10	4
PNNL-21990	Roll bonded LANL foil 3G60-CK-R1X6	L1: Zr-rich **(U)**	1.8-2.5 μm	6-8	4
		L2: speckled layer	0.9 μm	6-8	4
		L3: Mo_2Zr layer (C, P)	0.04-1.2 μm	6-8	4
		L4: 2-phase region	0.15-0.5 μm	6-8	4
PNNL-21990	Roll bonded Y-12 foil 3E67LA R9HT	L1: Zr-rich, wider than R1X4 and R9HW	3.8-5.8 μm	5-10	4
		L2: δ-UZr_2, Fe noted between layers 2 and 3	0.5-1.5 μm	5-10	4
		L3: blocky Mo_2Zr (P)	0.8 μm	5-10	4
		L4: 2-phase region (P)	0.8 μm	5-10	4
LA-UR-10-04294	Hot isostatic pressed (HIP) 52-1	L1: Zr rich layer	0.5-1.3 μm	55	5
		L2: uniform layer **(U)**	1.5 μm	55	5
		L3: blocky particles	0.5-1.3 μm	55	5
		L4: 2-phase eutectic	4.5-8.5 μm	55	5

Table 5. continued

Reference	Description	Interfacial Layer (P)=porosity, (C)=cracking, (U)=uniform	Thickness	Reference Image	Reference Number
LA-UR-10-01122	Friction bonded (FB) and HIPed FB 126	L1: Zr interlayer w/ ZrX (X=interstitial)	?		6
		L2: $\gamma U + UZr_2$	0.5-0.7 μm	76	6
		L3: $Zr_4Fe_2O_x$ phase grains	0.1-0.3 μm	76	6
		L4: $\alpha Mo + MoZr_2$ phase	0.4 μm	76	6
PNNL-24135		Image magnification insufficient to discern reaction layers			7
INL/CON-07-12224		Image magnification insufficient to discern reaction layers			9
Current Study	EDM interior slice U-10Mo casting	L1: Zr-rich **(U)**	0.4-0.7 μm	34	
		L2: thin layer	1.7-2.4 μm	34	
		L3: blocky ppt.(C)	0.1-1.5 μm	34	
		L4: U-rich two phase region	1.4-2.6 μm	34	
Current Study	EDM exterior slice U-10Mo casting	Zr did not adhere to fuel L1: blocky ppt. area (C)	0.7-1.7 μm	40	
		L2: U-rich two phase region	0.9-1.4 μm	40	

Characterization of Exterior Slice U-10Mo Foil

Images of the hot rolled exterior slice U-10Mo foil are shown in Figures 43 and 44. There is no zirconium cladding in Figure 43. A reaction layer is observed at the edge of the U-10Mo in the longitudinal section in Figure 44. The transverse section has a ragged edge with cracking in the U-10Mo fuel and an agglomeration of zirconium in the center of the image. The microstructure of the U-10Mo using DIC and polarized light is shown in Figures 45 and 46, respectively. Cracking within the U-10Mo was observed in the longitudinal section, seen in Figure 45. The grain structure appeared bimodal with some grains elongated, as expected for a rolled microstructure and comparable to images for the interior coupon (Figures 32-34). Polarized light images, in Figure 46, also show elongated grains in the transverse section.

Cracking at the edge of the cold rolled U-10Mo may have contributed to the lack of adherence of the zirconium layer, as seen in the longitudinal section in Figure 47. Cracking of the zirconium is also evident in the longitudinal sections of Figures 47 and 48. Zirconium fills an edge crack in the transverse section in Figure 48. The grain structure of the U-10Mo cold rolled exterior coupon is shown in Figures 49 and 50. A bimodal structure with elongated grains is

observed. Although the zirconium did not bond sufficiently to the U-10Mo fuel, a reaction layer was evident, as shown in Figures 51 and 52. Cracking at the interface of the blocky precipitate, identified in literature as Mo_2Zr,[3] was observed. The two-phase layer between the U-10Mo and the Mo_2Zr was also noted.

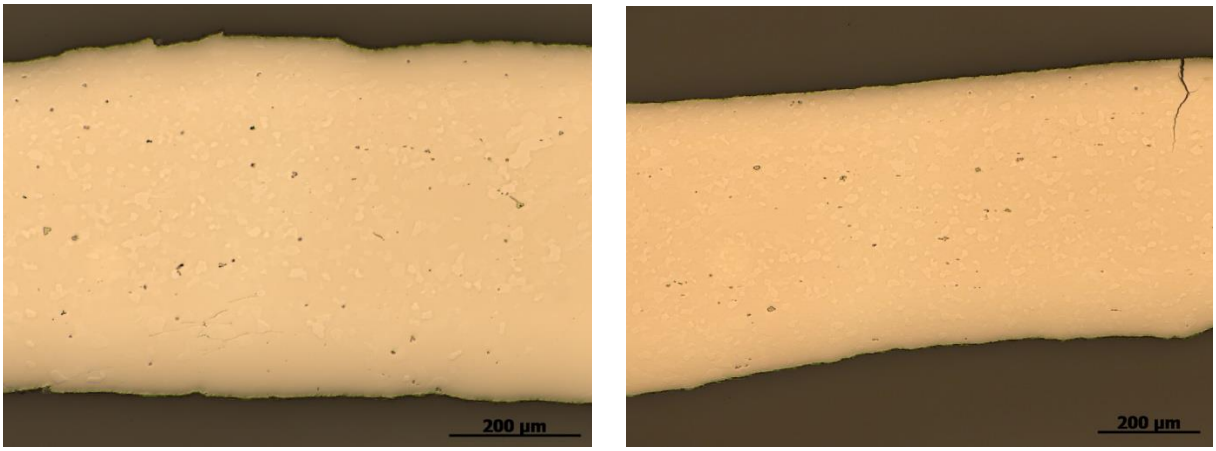

Figure 43. Images of hot rolled exterior U-10Mo slice showing no zirconium cladding on surface. The longitudinal section is on the left and the transverse section is on the right.

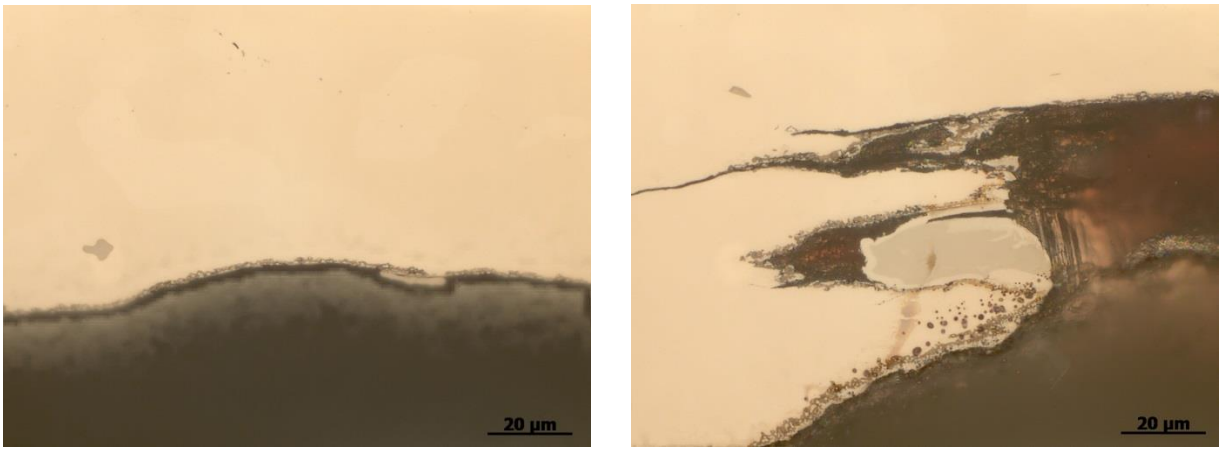

Figure 44. Higher magnification images of hot rolled U-10Mo exterior slice. The longitudinal section is on the left and the transverse section is on the right.

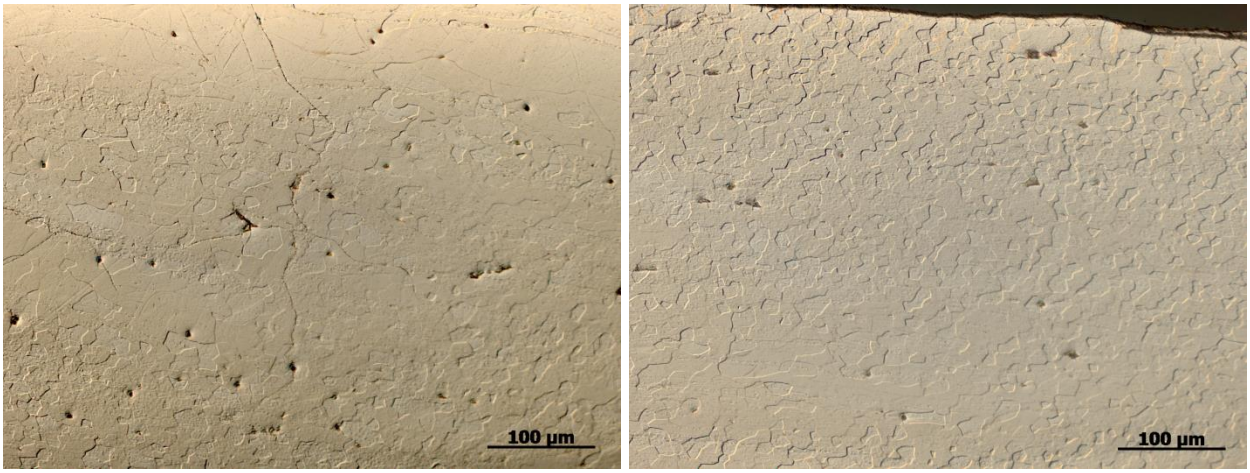

Figure 45. Differential interference contrast images of hot rolled U-10Mo exterior slice. Longitudinal section showing micro-cracking is on the left and the transverse section is on the right.

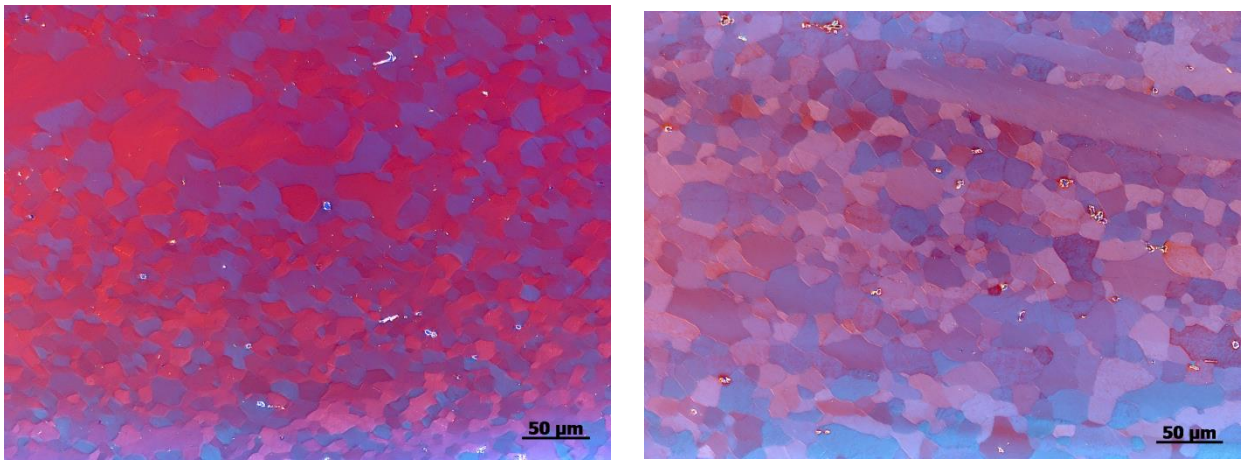

Figure 46. Polarized light images of hot rolled U-10Mo exterior slice. Longitudinal section is on the left and transverse section is on the right.

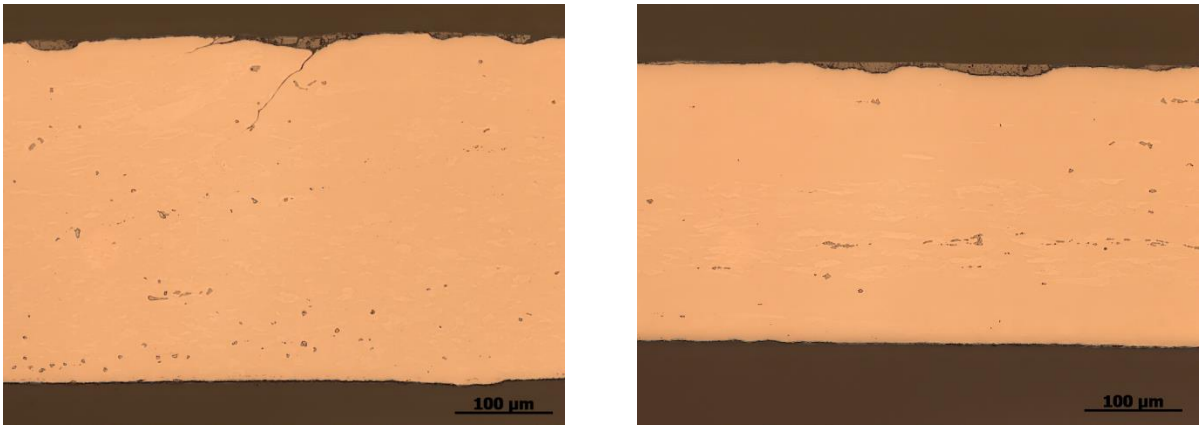

Figure 47. Metallographic sections of cold rolled exterior slice Zr-clad U-10Mo foil. Most of Zr adhered to the mild steel can upon removal. Longitudinal section is on the left and transverse section is on the right.

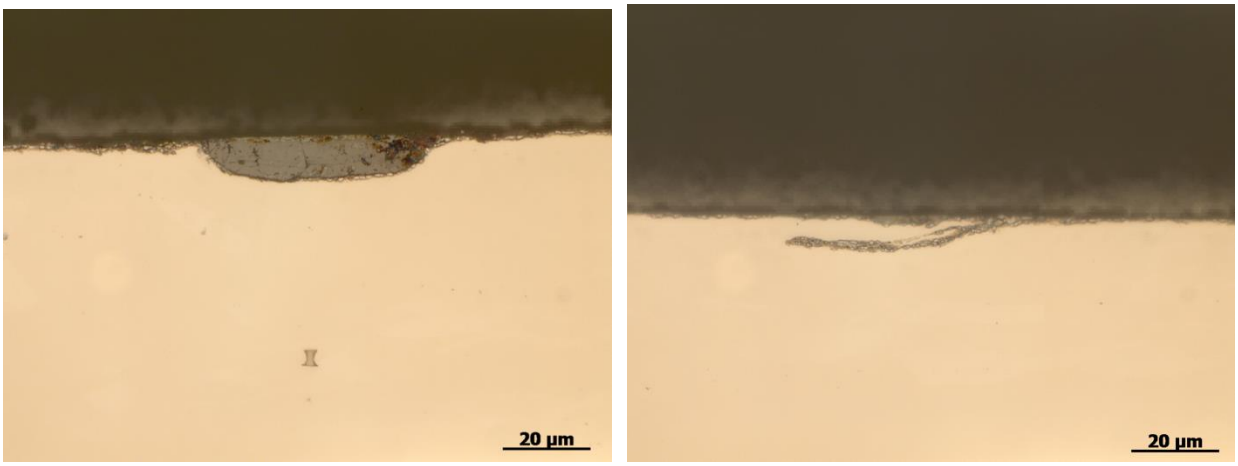

Figure 48. Metallographic sections of cold rolled exterior slice Zr-clad U-10Mo foil. Most of Zr adhered to the mild steel can upon removal. Longitudinal section is on the left and transverse section is on the right.

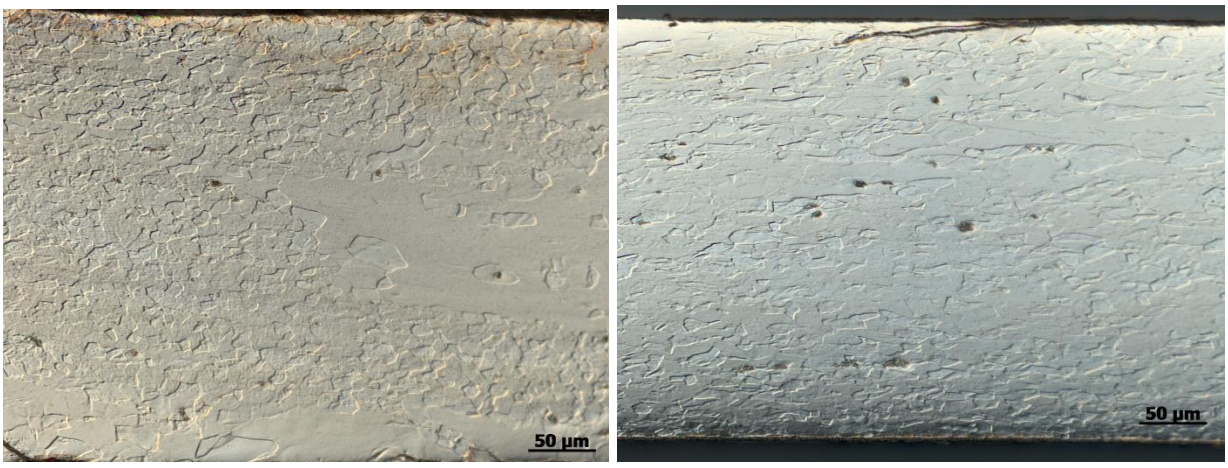

Figure 49. Differential interference contrast images of cold rolled exterior slice Zr-clad U-10Mo foil. Longitudinal section is on the left and the transverse section is on the right.

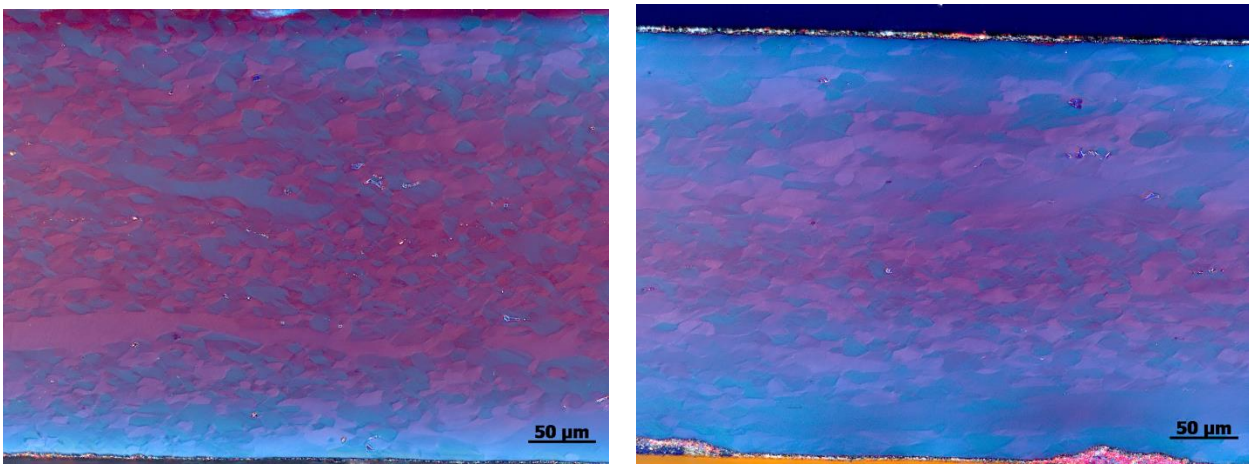

Figure 50. Polarized light images of cold rolled exterior slice Zr-clad U-10Mo foil. Longitudinal section is on the left and the transverse section is on the right.

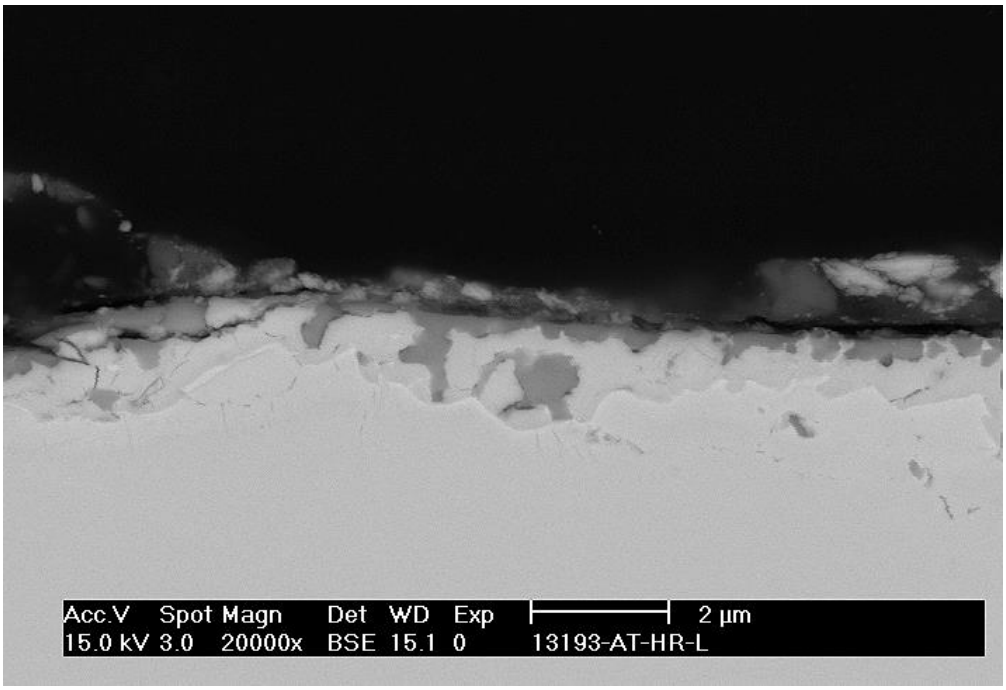

Figure 51. SEM image of hot rolled Zr-clad exterior U-10Mo slice.

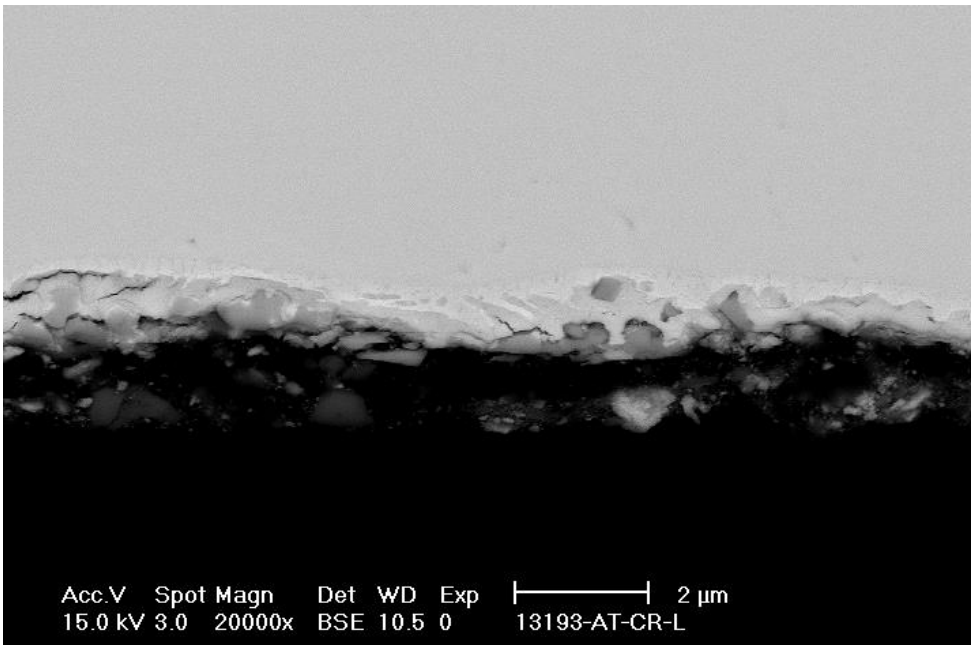

Figure 52. SEM image of cold rolled Zr-clad exterior U-10Mo slice.

Conclusions

The purpose of this study was to examine the feasibility of machining U-10Mo fuel using EDM. The kerf losses associated with the EDM were 0.3 mm, much less than that expected with conventional machining. The finish on the coupons was smooth and burr-free, eliminating the need for milling. Coupons showed no signs of distortion as a result of machining. The recast layer was easily removed by nitric acid. However, cracking was observed in both the interior and exterior coupons following cleaning. Two mild steel cans were assembled with zirconium foil covering the depleted uranium U-10Mo. One of the coupons in the steel can was from an interior U-10Mo slice while the other coupon came from an exterior slice with the surface adjacent to the mold milled 0.040" (1 mm) to remove any reaction layer with the mold. The cans were hot rolled and cold rolled. Metallography samples were machined from the foil to characterize the bonding between Zr and U-10Mo.

Variations in the thickness of the zirconium layer were greater in this study as compared to earlier studies. Reaction layers noted with the interior coupon were similar to those previously described in literature. Although, the eutectic layer was thicker than those documented earlier. Micro-cracking was observed at the Zr/U-10Mo interface in the presence of a reaction layer. The zirconium cladding did not adhere to the exterior slice U-10Mo. This problem may be associated with cracking of the exterior coupon.

EDM of U-10Mo is feasible and will result in minimal kerf losses upon machining. Processing optimization for achieving a more uniform zirconium layer would be required. It is unclear from this study whether an exterior slice coupon can be used for the fabrication of fuel foils and further trials would be beneficial.

Recommendations for Future Work

While this project demonstrated the feasibility of using EDM to machine fuel coupons, further studies need to be conducted to optimize machining parameters. Criticality concerns with the EDM deionized water bath need to be addressed. Fuel processing studies should be executed to refine the microstructure at the Zr/U-10Mo boundary. Based on this and previous studies, cracking is associated with coarse Mo_2Zr precipitates at the interface. Determining a threshold size for the Mo_2Zr precipitate as it relates to cracking would be a good first step.

References

1. E. B. Guitrau, The EDM Handbook, Hanser Publications, Cincinnati, Ohio (2009).
2. R. L. Edwards, M. A. Hill, J. D. Katz, D.E. Dombrowski, and R.K. Schulze, "Surface analytical measurements to certify cleaning methods for fuel element bonding operations: angle resolved XPS (ARXPS) measurements," Los Alamos National Laboratory report LA-UR-10-07345 (2010).
3. E. Perez, B. Yao, D.D. Keiser, and Y. H. Sohn, "Microstructural analysis of as-processed U-10 wt.% Mo monolithic fuel plate in AA6061 matrix with Zr diffusion barrier," *J. of Nucl. Mater.* 402 (2010) 8-14.
4. D. J. Edwards, C. H. Henager, R. M. Ermi, D. Burkes, A. L. Schemer-Kohrn, D. J. Senor, and N. R. Overman, "Characterization of U-Mo foils for AFIP-7," Pacific Northwest National Laboratory report PNNL-21990, (2012).
5. A. Clarke, P. Dickerson, R. Dickerson, R. Field, R. Forsyth, A. Kelly, C. Necker, P. Papin, and J. C. Foley, "Characterization report on hot isostatic pressed 52-1," Los Alamos National Laboratory report LA-UR-10-04294 (2010).
6. S. Casey, A. Clarke, K. Clarke, P. Dickerson, R. Dickerson, R. Field, R. Forsyth, T.G. Holesinger, A. Kelly, C. Necker, P. Papin, and J. C. Foley, "Characterization report on friction bonded 126 and hot isostatic pressed 52-1," Los Alamos National Laboratory report LA-UR-10-01122 (2010).
7. D. E. Burkes, P. J. MacFarlan, A. M. Casella, K.N. Pool, E. C. Buck, B.D. Slonecker, A. J. Casella, F.N. Smith, M. K. Edwards, and F. H. Steen, "Fuel thermophysical characterization project: year 2014 final report, Pacific Northwest National Laboratory PNNL-24135 (2015).
8. K. Hollis, N. Mara, R. Field, P. Dickerson, and T. Wynn, "Bond strength characterization of plasma sprayed zirconium on uranium alloy by microcantilever testing," International Thermal Spray Conference, May 21-24, Houston, Texas, (2012).
9. D.D. Keiser, J. F. Jue, and D.E. Burkes, "Characterization and testing of monolithic RERTR fuel plates," Idaho National Laboratory report INL/CON-07-12224 (2007).